

UNCLASSIFIED

AD NUMBER

AD917366

LIMITATION CHANGES

TO:

Approved for public release; distribution is unlimited.

FROM:

Distribution authorized to U.S. Gov't. agencies only; Test and Evaluation; DEC 1973. Other requests shall be referred to Naval Ship Research and Development Center, Attn: Code 1700, Bethesda, MD 20034.

AUTHORITY

USNSRDC ltr, 10 Feb 1975

THIS PAGE IS UNCLASSIFIED

THIS REPORT HAS BEEN DELIMITED
AND CLEARED FOR PUBLIC RELEASE
UNDER DOD DIRECTIVE 5200.20 AND
NO RESTRICTIONS ARE IMPOSED UPON
ITS USE AND DISCLOSURE.

DISTRIBUTION STATEMENT A

APPROVED FOR PUBLIC RELEASE;
DISTRIBUTION UNLIMITED.

AD 917366

NAVAL SHIP RESEARCH AND DEVELOPMENT CENTER

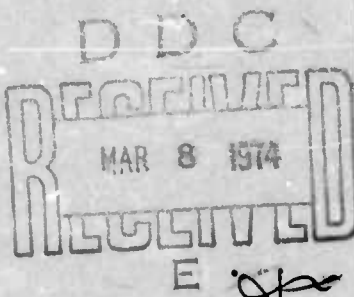
Bethesda, Md. 20034



EMPIRICAL DESIGN OF PERIPHERAL COLLISION PROTECTION STRUCTURE FOR THE ARCTIC SURFACE EFFECT VEHICLE

by

William E. Gilbert



Distribution limited to U.S. Government agencies only; Test and Evaluation Info., Dec 1973. Other requests for this document must be referred to NAVSHIRANDCEN, Code 1700.

AD NO. _____
DDC FILE COPY

STRUCTURES DEPARTMENT
RESEARCH AND DEVELOPMENT REPORT

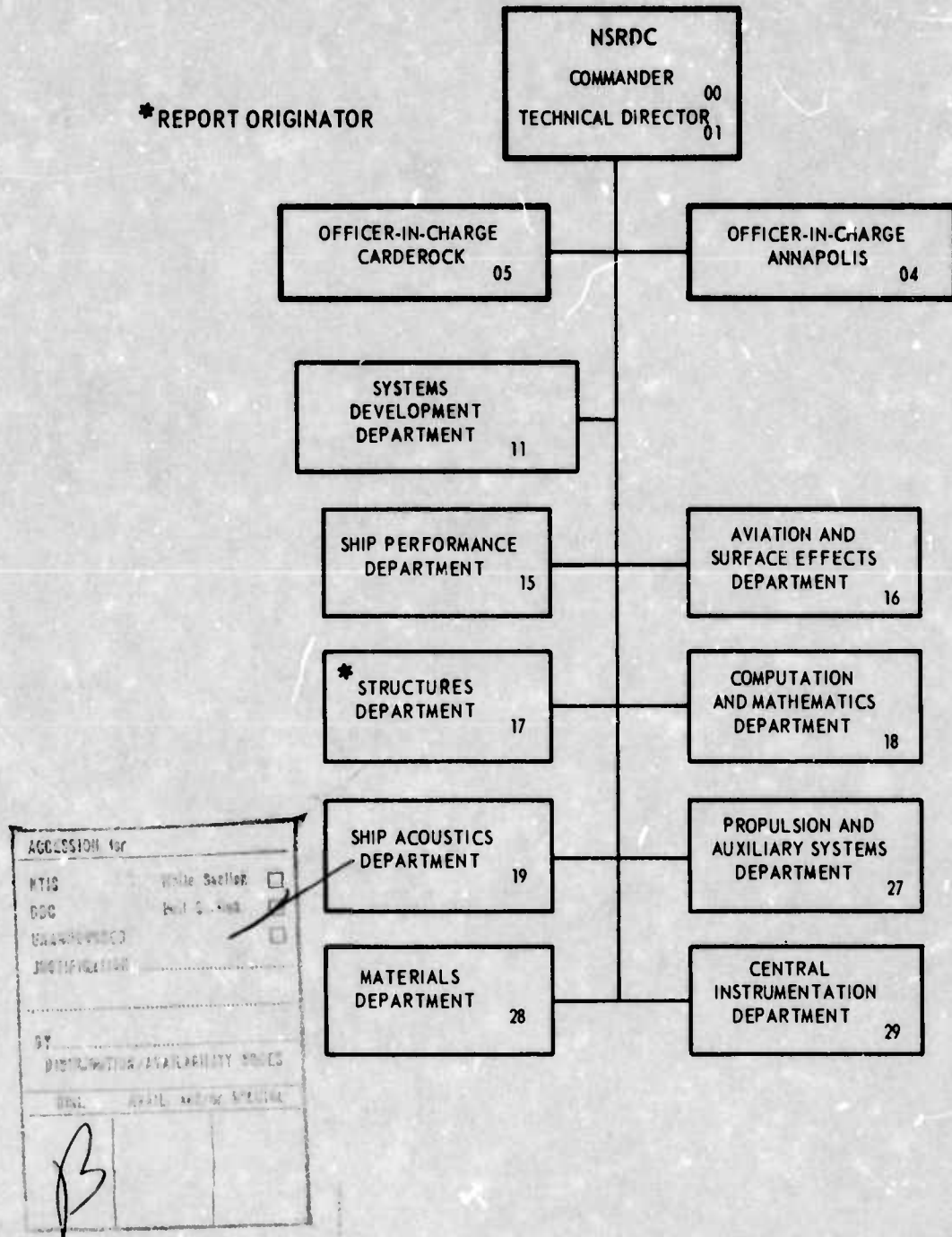
December 1973

Report 4232

The Naval Ship Research and Development Center is a U. S. Navy center for laboratory effort directed at achieving improved sea and air vehicles. It was formed in March 1967 by merging the David Taylor Model Basin at Carderock, Maryland with the Marine Engineering Laboratory at Annapolis, Maryland.

**Naval Ship Research and Development Center
Bethesda, Md. 20034**

MAJOR NSRDC ORGANIZATIONAL COMPONENTS



DEPARTMENT OF THE NAVY
NAVAL SHIP RESEARCH AND DEVELOPMENT CENTER
BETHESDA, MD. 20034

①

⑥ EMPIRICAL DESIGN OF PERIPHERAL COLLISION
PROTECTION STRUCTURE FOR THE ARCTIC
SURFACE EFFECT VEHICLE

⑨ Research and development rept.,

by
⑩ William E. Gilbert



Distribution limited to U.S. Government agencies only; Test and Evaluation Info., Dec 1973. Other requests for this document must be referred to NAVSHIPRANDCEN, Code 1700.

⑪ Dec [redacted] 73

⑫ 87 p.

⑬ NSRDC-
Report 4232

⑭ ARPA | Order-1676

+

1473
DN
387682

TABLE OF CONTENTS

	Page
ABSTRACT	1
ADMINISTRATIVE INFORMATION	1
COLLISION PROTECTION	1
THE PROBLEM	1
COLLISION PROTECTION PHILOSOPHY	5
EVALUATION OF COMPONENTS	8
GENERAL CHARACTERISTICS	8
CANDIDATE COMPONENTS	10
METHOD AND PROCEDURE	12
NSRDC BALLISTIC PENDULUM FACILITY	12
NSRDC DROP TOWER FACILITY	13
ANALYSIS OF DATA	15
RESULTS AND DISCUSSION	16
CIRCULAR CYLINDRICAL TUBING	16
SQUARE TUBING	19
FOAM CORE SANDWICH PANELS	19
BUMPER TUBES	20
DESIGN PROCEDURE AND CRITERIA	21
KEY PARAMETERS	21
LOAD DISTRIBUTION SYSTEM	25
STEPS IN THE DESIGN PROCEDURE	30
COMPUTER PROGRAM COLIDE	31
EXAMPLES	32
SUMMARY	33
ACKNOWLEDGMENT	34
APPENDIX A - EXPERIMENTAL DATA	57
APPENDIX B - SAMPLE TABLE OF PARAMETRIC DESIGN INFORMATION	71
APPENDIX C - LISTING FOR COMPUTER PROGRAM COLIDE	73
REFERENCES	76

LIST OF FIGURES

	Page
Figure 1 - Ideal Load Deflection Curve for Energy Absorption	35
Figure 2 - Kinetic Energy versus Craft Velocity	36
Figure 3 - Minimum Collision Protection Depth versus Limit Load for Various Craft Kinetic Energies	37
Figure 4 - Minimum Collision Protection Depth versus Impact Velocity for Various Numbers of Energy-Absorbing Elements	38
Figure 5 - Minimum Stopping Distance versus Impact Velocity for Various Limit Loads	40
Figure 6 - NSRDC Ballistic Pendulum Facility	41
Figure 7 - NSRDC Drop Tower Facility	42
Figure 8 - Inextensional Buckling in a Thin-Wall Cylindrical Tube	43
Figure 9 - Component Configuration with Two Energy-Absorbing Elements	44
Figure 10 - Base Support Modification for Multielement Configurations	44
Figure 11 - Experimentally Determined Efficiency Factors for the Tube in Inextensional Buckling	45
Figure 12 - Component Configuration with Four Energy-Absorbing Elements	46
Figure 13 - Inextensional Buckling in a Square Tube	47
Figure 14 - Typical Bumper Tube Collapse	48
Figure 15 - Crushing Force of the Cylindrical Tube as a Bumper	49
Figure 16 - Location of the Load Distribution System	50
Figure 17 - Shear and Moment Diagrams for the Load Distribution System	51
Figure 18 - Collapse of the Load Distribution System with Obstacle Contact between Energy-Absorbing Components	53
Figure 19 - Collapse of the Load Distribution System with Obstacle Contact on an Energy-Absorbing Component	53
Figure 20 - Collapse of the Load Distribution System under a Finite Sized Obstacle	54
Figure 21 - Total Weight of the Bow Collision Protection System versus Impact Velocity	55

	Page
Figure A.1 - Ballistic Pendulum Test of Two-Element Configuration	58
Figure A.2 - Drop Tower Tests of Two-Element Configurations	59
Figure A.3 - Drop Tower Tests of Four-Element Configurations	63
Figure A.4 - Drop Tower Test of Load Distribution System with Four-Element Configurations	65
Figure A.5 - Drop Tower Tests of Single-Element Configurations	66
Figure A.6 - Drop Tower Test of Foam Core Sandwich Panel	67
Figure A.7 - Drop Tower Tests of Cylindrical Bumper Tubes	68
Table 1 - Specific Energy Absorptions for Various Elements	11

NOTATION

A	Cross-sectional area
E	Modulus of elasticity (Young's modulus)
E_{cap}	Energy-absorbing capability
E_{craft}	Kinetic energy of a moving craft
E_{req}	Required energy-absorbing capability
E_e	Energy absorbed per element
F_c	Limit load or crushing force for a component configuration
F_e	Limit load or crushing force for an element
G	Geometric efficiency factor
g	Gravitational acceleration
I	Area moment of inertia
K	Cross-sectional efficiency factor or energy factor
k	Number of energy-absorbing components which act on each side of the obstacle contact area of the load distribution system
L	Length
L_c	Component length
L_{eff}	Effective length of a component
l	Span length between components
M	Mass

M_e	Moment at the first noncollapsing component in the load distribution system
M_p	Plastic moment
N	Number of components which collapse on each side of the impact area
N_c	Number of components which act in a collision
N_e	Number of elements per component
P	Impact load
R	Radius
R_e	Load on the first nondeforming component under the load distribution system
t	Thickness
V	Velocity
V_e	Shear at the extremity of the collapse region of the load distribution system
W	Weight
X_m	Maximum crush distance for the M^{th} component
α	Angle between energy-absorbing elements and the axis of symmetry of their component configuration
θ	Angle of plastic rotation of the load distribution system
σ_y	Yield stress

FOREWARD

The work reported herein represents part of a technology study for developing a total system for the operation of surface effect vehicles (SEV) in the Arctic. The overall program includes collision protection systems (as reported herein), obstacle detection systems, and improved maneuvering and control capabilities for the craft.

ABSTRACT

Collision protection for the Arctic surface effect vehicle (ASEV) was investigated and a collision protection philosophy developed for peripheral protection. Several peripheral protection schemes were evaluated and the most promising further developed and evaluated in a collision test program. A procedure is proposed for the design of discrete collision protection elements, and a computer program is documented which is a useful design tool when thin-wall tubes serve as the energy-absorbing elements.

ADMINISTRATIVE INFORMATION

Funding was provided by the Advanced Research Projects Agency (ARPA) under ARPA Order 1676, Program Code ON10, and administered by the Arctic Surface Effect Vehicle Program Office at the Naval Ship Research and Development Center (NSRDC). Preparation of this report was funded under Work Unit 1130-600.

COLLISION PROTECTION

THE PROBLEM

A surface effect vehicle (SEV) has been proposed in the range of 25 to 1000 tons gross weight for operation in Arctic regions at speeds up to 120 knots. The Arctic SEV is to be supported on a cushion of pressurized air partially contained by a flexible skirt system. In normal operations, the air cushion and skirt system will come in regular contact with minor obstacles. Because of the nature of the vehicle motion, the high operating speeds, the turning characteristics of the craft, and particularly the rough nature of the Arctic terrain, it is likely that the ASEV will encounter an obstacle which will contact more than simply the flexible skirt system. When the obstacle is too large for the vehicle to successfully clear and the craft is unable to stop or maneuver around the obstacle, collision will occur.

In a collision, the ice obstacle makes contact with the hard structure of the vehicle, i.e., with structures other than the flexible skirt system. As the velocity or kinetic energy of the craft drives the structure toward the obstacle, the impact loads increase until either the failure

load of the ice obstacle^{1, 2} or the yield limit load of the craft structure is reached. If the ice obstacle failure load is reached, then the ice fails in a brittle manner and no additional energy is absorbed by the obstacle itself. If the craft structure remains elastic, then after removal of the impact loading, the structure returns to its original position. It is possible that limited damage may result in accelerating the failed portion of the ice obstacle to the speed of the craft. This is likely to be very minor, however, and more severe collisions will control the craft design. When the ice obstacle failure load is greater than the yield limit load of the craft structure, it is the craft which fails. Fortunately, the craft structure can be more ductile than ice and brittle catastrophic failure avoided if energy of the collision is absorbed by plastic yielding of the structure or by other energy-absorbing systems carried by the vehicle.

Ideally there is a third collision category, one in which the ice obstacle failure load equals the yield limit load of the craft. The likelihood of encountering this situation in an actual collision is extremely small and since the craft structure is ductile, the consequences are not unlike those where the ice obstacle failure load is reached.

An actual collision will probably be a combination of the first two types. Since the ice obstacle will probably be irregular in shape, it appears likely that it will sustain local failures until the vehicle contacts the gross obstacle shape; then either the craft will begin to yield or the obstacle will fail catastrophically.

Obviously the most serious situation is one where the ice obstacle failure load is greater than the yield limit load of the vehicle. Since

¹Pounder, E. R., "Physics of Ice," Pergamon Press, New York (1965). A complete listing of references is given on page 76.

²Weeks, W. and A. Assur, "Mechanical Properties of Sea Ice," Cold Regions Research and Engineering Laboratory, Hanover, New Hampshire, Monograph II-C3 (Sep 1967).

such danger is a very real possibility, this situation should constitute the collision design condition.

In collisions where the ice does not fail and move from the path of the vehicle, the vehicle motion toward the obstacle must be halted. This does not necessarily mean that the vehicle must be brought to a standstill but rather that the component of the craft velocity toward the obstacle must be brought to zero. When the craft velocity vector is directly toward an obstacle such as in a head-on collision, then of course the full velocity must be reduced to zero. On the other hand, when the velocity vector of the craft is not fully directed at the obstacle, then only that velocity component so directed must be dissipated; the net effect of the collision is to change the direction of the craft velocity vector and reduce its magnitude.

The craft may be thought of as a mass moving toward the obstacle at a particular velocity. As such, the craft possesses a kinetic energy in the direction of the obstacle and that energy must be absorbed in some manner in order to accomplish the goal of collision protection. The magnitude of the kinetic energy is defined by the relationship:

$$E = 1/2 M V^2 \quad (1)$$

where E is the kinetic energy,

M is the mass of the craft, and

V is the craft velocity.

When the kinetic energy is absorbed, the velocity in that direction is zero. It is desirable that this energy be absorbed and not merely stored for later return to the craft. In the latter event, a velocity is imparted to the craft away from the obstacle, the craft essentially "bounces off" the obstacle, and secondary collisions may result.

The kinetic energy must either be plastically absorbed or be dissipated in some manner to prevent rebounding. The structure accomplishes this by doing plastic work. This means permanent deformation to structural components or "damage." Certain functions of the craft must be preserved in a collision to allow survival of the vehicle and completion of its mission. Systems which must be protected, for example, include propulsion

and lift, navigation and control, environmental, and primary structural systems. Of course additional systems may be included depending on the mission requirements. In any event, if these systems are to be protected, damage must be controlled so that it occurs outside the areas in which they are located.

Since many of the systems to be protected on an SEV lie within a central region on the craft, it is logical to define a region where damage will be allowed (henceforth referred to as the collision protection region) as all of a structure external to the location of critical systems. Where a critical system is located near the periphery of the vehicle, it will probably be necessary either to move the system or to add some protection structure external to the system in that area. A system at or near a potential area of obstacle contact is vulnerable to direct damage as a result of contact with the ice obstacle and/or to shock-induced damage as a result of the collision motions since decelerations in the contacted regions may be quite high.

Because of the nature of the vehicle motion, the bow extremity of the structure is the area most likely to be involved in collisions. Such collisions are likely to be of the "head-on" type and high impact energies may be expected. Since the craft is not a tracked vehicle and side slips in cross winds, in crossing transverse slopes, and in negotiating turns, the side extremity structure is also potentially vulnerable to collision. A study of craft motions in various standard maneuvers should reveal the relative vulnerability of the side structure to collision. The stern extremity structure is also potentially susceptible to collision, but impact velocities there are likely to be quite low and therefore the relative vulnerability of the stern structure is probably much lower than at the bow extremity. The entire underbody structure of the craft is also a likely collision zone in the event that the craft descends onto a pinnacle either following a "ski jump" or in a power loss where the cushion pressure is suddenly lost.*

*A "ski jump" is a maneuver where the craft is given enough upward velocity by the terrain (such as in a ramp) to momentarily rise sufficiently to clear an ice pinnacle in its path. On descent, the obstacle is a hazard to the underbody.

Basically, the problem of collision protection may be stated as the design of lightweight energy-absorbing structures or components which can be placed in the collision protection region to serve as a buffer between ice obstacles and the critical vehicle systems. The collision protection regions are the extremity structure at the bow, the sides, and--to a lesser extent--the stern as well as the underbody structure forward of and beneath critical systems.

COLLISION PROTECTION PHILOSOPHY

The basic collision protection philosophy for the ASEV is to confine collision damage to the collision protection regions and to limit their transmittal of loads to the primary structure to values less than those which will damage it.

The structure designed for the collision protection region may serve a number of functions, e.g., skirt support structure, air plenum to feed the air cushion, support structure for expendable stores and equipment, etc. However, the main function of this structure must be collision protection, and its design must be controlled by collision protection criteria.

To be most efficient, the collision protection structure must deliver a constant force through the entire crushing distance and this force should be just slightly less than the capability of the primary structure to accept loads in that area without damage. It may be desirable to add a factor of safety on this limit load to ensure against damage to the primary structure. Another design consideration is the motion environment imposed on the crew and equipment^{3, 4} during a collision. Since man and equipment are sensitive to accelerations on the order of 10 g, the collision loads must not impart gross craft accelerations of that magnitude. This is not a problem for large, massive craft of low limit load

³Hirsch, A. E., "Man's Response to Shock Motions," David Taylor Model Basin Report 1797 (Jan 1964).

⁴Mahone, R. M., "Man's Response to Ship Shock Motions," David Taylor Model Basin Report 2135 (Jan 1966).

capability since sufficient force to impart high accelerations cannot be tolerated in the design of the collision protection structure. For lighter craft, however, and for massive craft of high limit load capability, a cutoff in limit load design value may occur because of the acceleration criterion. In other words, the loads transmitted to the primary structure of the vehicle by the crushing energy-absorbing structure may be required to be less than the capability of the primary structure to accept that load in order to maintain the deceleration environment within tolerable limits. This criterion may be particularly evident in underbody protection where space is more at a premium. Collision protection depth is limited and thus the impact loads required to absorb a given amount of energy will be higher.

A collision protection structure should be designed for a particular design condition, that is, a particular craft weight and velocity. Inherent in the design philosophy presented here is the capability and desirability of the collision protection structure to offer protection at other than the design conditions. The protection system should function at impact velocities below the design collision velocity. Most systems will offer this feature automatically but some may not. For example, an improperly designed fluid dispersal system (a system that uses shock absorbers as the energy-absorbing elements) may not have the same energy-absorbing characteristics at low as at higher velocities.

It is most important that the collision protection structure be capable of functioning during collisions that are more severe than the design collision. This means that the load transmitted to the primary vehicle structure by the collision protection structure should be independent of the impact velocity for a reasonable range of velocities. The collapse mechanism should remain stable throughout the impact, whether or not the impact is at design conditions. The benefits of such a criterion is that beyond its design range, the collision protection structure serves as a damage-inhibiting structure. If the Arctic vehicle is involved in a collision more severe than the design collision, the protection structure will extract the full energy of the design collision from the energy of the real collision, leaving less energy available to damage the primary craft structure and other critical vehicle systems.

If such a collision protection philosophy is not followed, the consequences may be a structure which collapses in a less efficient manner, thus absorbing less energy and resulting in more damage to important vehicle systems. A more serious possibility is that the energy-absorbing components may transmit a higher loading to the primary craft structure than it is capable of accepting. This will result in immediate transfer of the collision energy to the very systems the protection system was designed to protect. This consequence is potentially very dangerous since the collision protection structure is then essentially bypassed by the collision energy and the full brunt of the impact is felt by the main craft.

The collision protection region, then, is viewed as an energy-absorbing buffer zone between unyielding ice obstacles and the primary craft structure and its critical systems. The component members of this buffer zone must collapse in such a manner that they remain stable throughout their collapse and are therefore able to absorb energy through the full collapse distance. The components must collapse in such a way as to limit the load transmitted to the rest of the craft. Since energy absorption is the prime purpose of the components and since weight is so critical on a vehicle of this type, the components must absorb energy in the most efficient manner possible. The ideal energy absorber has a force deflection curve as shown in Figure 1. If possible, the components of the collision protection structure should be either restorable to their undeformed shape (e.g., by reinflation of an air bag or restoration of a fluid shock absorber) or replaceable either in the field at the collision site or back at a home base where more elaborate facilities are available.

Components may be discrete units, such as crushable metallic structural elements or fluid shock absorbers, or they may be semicontinuous, such as a segmented air bag. In either case, it is necessary to determine how many components act in an obstacle collision. If the collision is head-on into an ice ridge that is wider than the width of the craft, then obviously all the bow extremity components will absorb energy. On the other hand, if the collision is with an ice pinnacle just large enough to prevent failure of the pinnacle, then a relatively small number of components will be involved. In some instances, it is possible to design a load distribution system which is installed external to the energy-absorbing components and

which distributes the collision loading to a greater number of components. It is unlikely, however, that as many components can be involved in collision with a discrete obstacle as in one with a very large obstacle such as an ice ridge.

Since the total energy absorbed in any collision is directly related to the total number of energy-absorbing components involved, the ability of the craft to survive a collision depends on the size of the ice obstacle. The smaller the obstacle, the more concentrated the collision impact and the fewer the number of components available to absorb the energy. In other words, collision vulnerability is an inverse function of obstacle size. This is perhaps a paradox in that the small obstacle is a more severe hazard due to its penetrating capabilities. Since the energy-absorbing capability is a direct function of the number of components and the collision velocity is a square function of the impact energy, the velocity at which a given craft is vulnerable to collision is related to the square root of the number of involved energy-absorbing components and thereby discontinuously to the square root of the obstacle size.

The most dangerous form of collision, then, is one with an ice obstacle just large enough to survive under the loads imposed by the collapsing collision protection structure. Such an obstacle would be small enough to involve a minimum number of components and the total absorbable kinetic energy would be relatively low.

A statistical study of ice obstacles of sufficient size to pose a collision hazard should reveal whether this optimum size obstacle occurs often enough in the Arctic to warrant making this collision mode the design collision. Certainly studies of this type are needed to determine safe speeds for SEV's operating in specific Arctic regions or specific types of terrain.

EVALUATION OF COMPONENTS

GENERAL CHARACTERISTICS

The energy-absorbing components of a collision protection structure must be stable through their collapse, have the ability to limit the load transmitted to the primary craft structure, be insensitive to collision

velocity within the likely range of vehicle operating velocities, be light in weight, and be restorable, repairable, or replaceable.

The Arctic SEV is a weight-sensitive structure and therefore every pound of material in the collision protection regions must function as efficiently as possible. In addition, the speeds at which the proposed craft will operate and the weight of the craft contribute to extremely high kinetic energies. Figure 2 indicates energy as a function of velocity for various craft weights. The magnitude of these energies dictates that the collision protection structure must not only be efficient weightwise but that it must also absorb tremendous amounts of energy in a collision.

Additional constraints may arise when the collision protection structure is used for other functions as well. For example, if the collision protection region is to be used as an air plenum to supply the skirt bags and the air cushion, then there must be a considerable portion of open passage to allow air flow past the components. If the components are to be used as structural elements such as in support of the flexible skirt system, then sufficient strength and stability must be built into the component configurations to accept those loads. In such cases, however, the energy-absorbing function must have prime priority in design; no changes should be made which might impede the process of energy absorption or deliver loads to the primary craft structure greater than the limit load. It should also be recognized that the collision protection region and its components are viewed as expendable in a collision. Therefore, any collateral function served by the protective structure before a collision may not be served following it without a certain amount of on-site remedial action.

The assumption that the element is an ideal energy absorber, i.e., that the force deflection curve is as illustrated in Figure 1, enables a few general comments to be made regarding energy-absorbing elements. The absorbed energy, then, is the limit load F_c times the crushing distance X :

$$E_{craft} = 1/2 \frac{W}{g} v^2 = N_c F_c L_{eff} \quad (2)$$

where W is the weight of the craft,
 E_{craft} is the energy,
 g is the acceleration due to gravity,
 V is the impact velocity,
 N_c is the number of components assumed to fully act,
 F_c is the limit load delivered by each component, and
 L_{eff} is the effective component length of the stopping distance.

Equation (2) is the energy balance in a successful stop in a collision where the velocity of the craft is brought to zero by using the full capability of the protection system.

If the craft collides head on with a very large barrier, an ice ridge for example, the minimum collision protection depth as a function of limit load for various craft kinetic energies is as presented in Figure 3. This plot assumes that 44 components are acting. A craft kinetic energy of 3.0×10^4 kip-ft corresponds to a 500-ton craft moving at 26 knots or a 25-ton craft moving at 116 knots.

The effect on required collision protection depth of the number of components assumed to be absorbing the energy is illustrated in Figure 4a for a limit load of 60 kip and in Figure 4b for a limit load of 100 kip. Figure 5 illustrates the effect of the limit load on required collision protection depth for a 500-ton craft and 44 involved components.

CANDIDATE COMPONENTS

Many candidates have some or all of the characteristics needed to serve as a component of the collision protection structure. Gilbert⁵ has compared air bags, thin wall tubes in inextensional axial buckling, fluid dispersal shock absorbers, foam core sandwich panels, energy-absorbing steering columns, and torsional tubes on the basis of energy absorbed per

⁵Gilbert, W. E., "Collision Protection for the Arctic Surface Effect Vehicle (ASEV)," NSRDC Report 3885 (Feb 1973).

unit weight or specific energy absorption. Table 1 reveals that the greatest potential is offered (in descending order) by an air bag, axial inextensional buckling components, the rod pulled through a die, and an inverting tube.

TABLE 1 - SPECIFIC ENERGY ABSORPTIONS FOR VARIOUS ELEMENTS
(From Gilbert⁵)

Type of Element	kip-ft/lb
Axial Inextensional Buckling	
Buckling of Planar Tube Components	
(Realized)	6.55
(Potential)	12.0
Rods Drawn Through a Die	6.0
Bumper Tubes	1.5
Fluid Dispersal Shock Absorbers	0.2
Foam Core Sandwich Panel	0
Air Bag	10.0*
GM Steering Columns	0.62
Inverting Tubes	3.0
Torsional Tubes	1.13
*Ideal conditions.	

Since the tube in axial inextensional buckling⁶ and the air bag⁷ appear to offer the most promise, they were selected as the major items for additional study. The air bag investigation was completed in June 1972 and

⁶Goppa, A., "On the Mechanism of Buckling of a Circular Cylindrical Shell Under Longitudinal Impact," General Electric Company, Missile and Space Vehicle Department, Technical Information Series R60SD494 of the Space Sciences Laboratory (1960).

⁷Howe, J. T., "Theory of High-Speed-Impact Attenuation by Gas Bags," NASA, Ames Research Center, NASA-TN-D-1298 (Apr 1962).

has already been reported.* The present report documents the analytical and experimental investigation of the tube in inextensional buckling, in particular thin-wall cylindrical tubes since those shapes appeared to be the most efficient. A few tests were also run on square tubing because of its possible advantages for fabrication. These results are also presented in this report together with results of several tests to evaluate the performance of a foam core sandwich panel loaded in the plane of the panel.

METHOD AND PROCEDURE

The initial tests were conducted on a small scale in the ballistic pendulum facility. When the energy requirements for the impact tests exceeded those available on the ballistic pendulum, the tests were performed in the drop tower facility. Both facilities are located at the Naval Ship Research and Development Center.

NSRDC BALLISTIC PENDULUM FACILITY

The ballistic pendulum facility (Figure 6) consists of two heavy cylinders suspended from an overhead beam. The cylinders are solid steel and are oriented end to end. Both are suspended at the same height and in such a manner that when either cylinder is swung along the line of the impact, it does not rotate. The structural component to be evaluated is mounted on the end of Cylinder A, the hammer. Cylinder A is drawn back away from Cylinder B, the anvil, to the proper height and released. The potential energy stored in the pendulum at release is returned in the form of horizontal kinetic energy at the time of impact with the stationary pendulum.

The response of the structural component is measured by accelerometers. One is located on the nonimpacting face of each of the two cylinders. They

*Reported informally in June 1972 by W. R. Conley as enclosure 1 (The Use of Gas-Filled Bags for Impact Attenuation on the Arctic Surface Effect Vehicle) to NSRDC letter Serial 72-172-286.

are oriented to sense accelerations along the line of impact or along the axis of the cylinders. The cylinder which acts as the hammer weighs about 837 lb and the anvil cylinder weighs about 633 lb.

Since the only forces that act horizontally on the mass of the cylinders are a direct result of the crushing of the structural component between the cylinders, the crushing force is determined by multiplying the measured acceleration (or deceleration) of a given cylinder by its mass. Since the same force acts on both cylinders of the ballistic pendulum, the same result should be obtained by multiplying each cylinder mass by its acceleration. Accordingly, a comparison of their records provides a check on the accuracy of the data.

Six tests were conducted at drop heights for the impacting pendulum that ranged from 16 to 58 in. above the stationary pendulum. This corresponds to an impact velocity range of 9.2 to 17.6 ft/sec and an impact energy range of 1.1 to 4.0 kip-ft. The principal reasons for the ballistic pendulum tests were to observe the phenomenon of inextensional buckling in cylindrical tubing and to predict on a small (inexpensive) scale the characteristics which make a tube buckle inextensionally rather than by gross buckling (Euler buckling).⁸

The ballistic pendulum is capable of delivering a maximum impact energy of about 4.0 kip-ft. It is necessary to attain higher impact energies to test larger models and models of longer length or heavier wall thicknesses.

NSRDC DROP TOWER FACILITY

The drop tower facility (Figure 7) offers the advantage of higher drop heights with about the same impacting mass, and therefore, higher impact energies. It is approximately 50 ft high and has a potential drop distance of about 45 ft. The structural components tested were positioned

⁸ Timoshenko, S. P. and J. M. Gore, "Theory of Elastic Stability," Second Edition, McGraw-Hill Book Company, New York (1961), pp. 1-8.

on a nonyielding baseplate at the foot of the drop tower. The facility allows the impacting mass to be raised to the desired height above the component and released electrically. The mass is kept aligned and guided toward the model by two vertical cables. Two accelerometers located on the nonimpacting side of the mass are aligned to record accelerations (decelerations) along the line of the impact. Both accelerometers should read the same motions; duplication is employed only to avoid loss of data and as a check on accuracy. Since the motion of the impacting mass is vertical, the acceleration due to gravity acts along the same line as the crushing forces. This motion is easily included by establishing as a datum the accelerometer output just prior to impact. Since the only other vertical forces on the impacting mass are the crushing forces, these are obtained by multiplying the measured accelerations by the impacting mass.

For several tests, a velocity measurement was made just prior to the time of impact in order to determine whether the guidance cables had altered the energy of the impacting mass on its path to the model. The mass was allowed to strike and break two lead contacts a known distance apart and located just above the structural component to be evaluated. As the mass struck each of the leads, an electrical closure was obtained and a blip was recorded on magnetic tape. The velocity was calculated by knowing the time between the recorded blips. It was found that the velocity was extremely close to the free-fall velocity and, therefore, no significant energy loss is ascribed to the guidance cables. In fact, after all of the early test drops indicated no energy losses, the velocity measurement was discontinued.

The fact that no significant energy losses were present due to the guidance cables allowed a check of the accelerometer calibrations. Since the drop vehicle drops a known height, the change in potential energy and therefore the change in velocity through the collision is known. When the accelerometer record is integrated over the time of collision, the velocity change should correlate with the calculated velocity change if the accelerometer calibration is correct. When this comparison was made, the experimental data were found to be within 2 percent of the theoretical velocity change. This is well within the accuracy of the recording equipment and therefore it is assumed that the accelerometer calibrations were good.

Drop heights utilized on the tower facility ranged from 1.5 to 42.8 ft. Impact velocities therefore ranged from 9.8 to 52.5 ft/sec. The impacting weight was 729 lb and so the impacting energy ranged from 1.09 to 31.2 kip-ft. Most of the tests on the axially loaded cylindrical tubing were made at the higher end of the energy range.

To date, 57 drop tests have been performed. Many were designed to evaluate different configurations and dimensions of thin-wall tubes in inextensional buckling. Several were run to evaluate the axially loaded foam core sandwich panel. The remainder were evaluations of thin- and thick-wall tubes loaded perpendicular to their longitudinal axes in order to evaluate tube suitability as a replaceable, low-energy bumper for the ASEV. One test was run on a composite configuration to evaluate a load distribution scheme.

ANALYSIS OF DATA

Signals from the two accelerometers were amplified and recorded on magnetic tape, processed through a digitization process, and plotted by the CDC 6700 computer system at NSRDC. Playback of the records on an oscilloscope provided preliminary data.

High-speed photographic coverage was used on selected tests made in both facilities to allow a detailed analysis of the crushing phenomenon.

To derive force histories, the acceleration-time histories (in g) were simply multiplied by the weight of the cylinder on which the accelerometer was mounted. In the drop tower tests, both accelerometers were mounted on the same cylinder (729 lb). In the ballistic pendulum tests, however, the accelerometers were mounted on different cylinders of different weights. Therefore, a weight of 837 lb was used to derive force from the accelerometer on the impacting cylinder (hammer). A weight of 633 lb was used to convert the accelerometer record of the impacted cylinder (anvil). The two force-time histories should be identical, however, since the crushing model imparts the same force to each cylinder, and the test data support this fact.

RESULTS AND DISCUSSION

In all cases, both accelerometer channels indicated the same force-time history within about 5 percent. Selected detailed results from the pendulum and drop tower tests are presented in Appendix A. In the interest of space and to avoid redundancy, only one of the accelerometer records from each type of test is presented.

CIRCULAR CYLINDRICAL TUBING

The major portion of the data concerns axial inextensional buckling of the thin-wall extruded aluminum tube. Single tubes were tested to determine the characteristics of the buckling phenomena and, subsequently, configurations of tubes were tested to define their interaction in an impact condition. Figure 8 illustrates a single tube following impact. The buckling pattern is characteristic of axial inextensional buckling. A typical two-element configuration is shown in Figure 9.

Where impact testing was conducted on two or more element configurations, it was found that when inextensional buckling occurred near the base of the tube, its lateral stability was lost or reduced because the buckled segment was not capable of carrying significant lateral shear loading. This problem was remedied by supporting the base of each element on an inclined surface; see Figure 10. The angle causes the load transfer to the base to be oriented principally along the tube axis, thus reducing the requirement for shear load capacity in the element. Of course, since the angle between the tube and the base changes as the configuration is progressively crushed, it is necessary to bias the angle somewhat.

Data from the crushing of thin-wall tubing indicate that the tube will either buckle in the fundamental (Euler) mode or in the inextensional buckling modes. The geometry of the tube determines the buckling mode. The fundamental Euler buckling load is computed using the Euler equation:

$$F = \pi^2 \frac{EI}{L^2} \quad (3)$$

Note that the column length used in Equation (3) is for a pin-ended column. This is necessary since the column is essentially pin-ended after the initial formation of inextensional buckling and Euler buckling may still occur after the start of inextensional buckling.

The buckling load for the more local effect of inextensional buckling is defined by cross-sectional geometry. Experimental results indicate that this load may be defined as a function of the ratio of the tube radius R to the wall thickness t , the cross-sectional area A , and the yield stress of the material σ_y . The crushing load for inextensional buckling, then, may be expressed as:

$$F_e = K \sigma_y A \quad (4)$$

where K has been found experimentally to be

$$K = 0.9107 e^{-0.0523 R/t} + 0.16 \quad (5)$$

Note that this load is not the critical load which starts the inextensional buckling process but rather the load which crushes the tube axially in the pattern prescribed by the buckling. If this crushing load is greater than the critical Euler buckling load, then the tube will buckle in the Euler mode. On the other hand, if the crushing load is less than the critical Euler load, the tube will crush in the inextensional buckling pattern.

Much work has been done on defining the loads necessary to start inextensional buckling; these loads have been shown to be functions of the impact velocities.⁶ For the velocity range of interest, however, their magnitude is unimportant. The impulse associated with them is not sufficient to cause Euler buckling, and it appears that the buckling pattern is consistent within the velocity range of interest. Note that whereas Euler buckling is gross buckling and affected by the overall length of the column, inextensional buckling is a local effect and is a function of local geometry. As such, the column length has no affect on inextensional buckling crushing loads.

The equation for K has been determined for R/t ratios from about 15 to about 80. It is anticipated that inaccuracies in K can be expected below an R/t value of about 10. For very large values of R/t , the tube

appears to be more like a shell than a tube. The buckling of thin shells has not been studied here, and it is recommended that the equation for K be applied only for R/t ratios between 10 and 120.

Factor K is referred to as an efficiency factor or energy factor, since it defines the proportion of the material in a cross section which exceeds the yield stress and which plastically absorbs collision energy. Figure 11 presents the experimentally determined value of the efficiency factor as a function of the ratio R/t . This curve shows that the efficiency is higher for small-diameter, thick-wall tubes than for larger diameter, thin-wall tubes. This defines the collapse (crushing) load for a given cross section in inextensional buckling. To evaluate the energy-absorbing capacity for a configuration or for a structural element, it is necessary to compute the distance over which that crushing force will act.

The accelerometer records indicate that the crushing force for the tube is essentially a constant force. The same tube section tested on a range of drop heights, and therefore a range of velocities, indicates no variance of the crushing force with velocity. Also, the data are repeatable; if the same test is run again, the results are identical.

Since the tube exhibits a constant crushing force during inextensional buckling, its energy-absorbing capability is defined by the crushing force times the crushable length. In the case of a single tube aligned with the impacting surface, the crushable length is theoretically the entire length of the tube. Actually, this is not the case since the completely crushed tube does not have zero length. The difference is not important, however, since the tube will usually be used in a configuration with other tubes to form an energy-absorbing component. The geometry of the component, then, will define the crushable length of individual tube elements. The component illustrated in Figure 12 was analyzed by using limit analysis techniques; the effective crushable length for total energy absorption capability was found to be equal to 67 percent of the component length. The crushable length of the element is related to the crushable length of the component through the component geometry.

SQUARE TUBING

Square tubing (Figure 13) was investigated as an alternative to cylindrical tubing because of possible fabrication advantages for the flat surfaces of the square tubing. Several tests were conducted for two different square tube cross sections. When a cross-sectional efficiency factor was computed from the experimental results, it was found that the square tube efficiency was considerably less than that of a comparable cylindrical tube. If the comparison is for an actual element design on the basis of equal energy-absorbing capability and equal crushing force, the difference between the two cross sections is not as great as indicated by their relative cross-sectional efficiency factors. A 4-in. square tube designed with a 1/8-in. wall was 24 percent heavier than a cylindrical tube designed to absorb the same energy at the same crushing force.

Obviously, this comparison is valid only for the cross sections where the comparison was made. Further testing is required in order to extend these results to a greater range of square tube cross sections.

FOAM CORE SANDWICH PANELS

A few drop tower tests were conducted to investigate the energy-absorbing potential of foam core sandwich panels. These tests were undertaken because transverse bulkheads sometimes extend to the periphery of the craft on an ASEV and Euler buckling of these panels must be avoided in order to attain efficient energy absorption. (Euler buckling of a panel with subsequent formation and distortion of plastic hinges is a very inefficient method of energy absorption.) It was reasoned that if very thin metallic walls were used with a weak filler material such as low density styrene foam ($2 \text{ lb}/\text{ft}^3$), the filler might function only as a spacer between the thin walls and thus lend stability. The walls might then buckle locally rather than in the Euler mode. Under the impact loading of the drop test tower, the foam core essentially strengthened the panel in plane due to the dynamic behavior of the foam enclosed between the aluminum sheets. The net result was Euler buckling of the panel with little or no energy absorption. When loading is rapidly applied to styrene foam, especially enclosed foam, the foam is effectively more rigid than statically

loaded free foam. When this happens, the panel crushing load is higher, and if the crushing load exceeds the Euler critical buckling load, the panel will buckle in the Euler mode.

Since the panel buckled fundamentally, it was known only that the crushing load was greater than the fundamental buckling load. Subsequent impact tests were run on foam core sandwich panels with shorter element lengths in an attempt to increase the critical fundamental buckling load above the crushing load, but these efforts were unsuccessful. Accordingly it was concluded that: (1) the foam is a significant part of the element and cannot be analyzed as a filler material alone; (2) because of the effects of the foam, the panel must be very thick and short to prevent fundamental buckling; and (3) the foam core sandwich panel in the proportions originally envisioned is ineffective as an energy-absorbing element.

BUMPER TUBES

Another type of energy-absorbing element investigated experimentally was the extruded tube impacted side on, causing the cross section to deform from the original circular shape to an oval shape and finally to a completely flattened oval. This type of element is potentially useful as a low velocity bumper. The element would be located external to the major energy-absorbing configurations and was evaluated only as a device to absorb the energy of incidental (very minor obstacle) contacts. The element has the advantage of being easily accessible for replacement.

Perrone⁹ has evaluated the energy-absorbing characteristics of steel tubes impacted in this manner. A few drop tower tests were run in the present study to extend the evaluation to aluminum tubes. Figure 14 illustrates the mode of the crushing, and the curve of Figure 15 relates the crushing force to cross-sectional dimensions of the tube and the yield stress of the material. The test data are included in Appendix A.

⁹Perrone, N., "Impulsively Loaded Strain-Hardened Rate-Sensitive Rings and Tubes," Report 10 under National Science Foundation Grant GK782, Catholic University of America (Apr 1969).

DESIGN PROCEDURE AND CRITERIA

KEY PARAMETERS

A peripheral collision protection structure is designed by first evaluating the allowable loads which it can transmit to the primary craft structure without causing damage.

An element that is capable of absorbing energy at a relatively constant rate is the most efficient form of collision protection since the crushing force is relatively constant and the allowable or design crushing force can be higher. The design crushing force must be equal to the peak crushing force and less than the force capable of causing primary structural damage. It is obvious, then, that if the crushing force is a constant through the collision, full advantage may be taken of the ability of the primary structure to carry load.

The selection of a design collision or a set of design collisions must be based on the operational characteristics of the ASEV and the hazards of the region of operation. Specifically, obstacle sizes must be selected since they represent a key parameter in determining the number of collision protection components which absorb energy in a given collision. A small obstacle that can accept the loads delivered to it by the crushing energy-absorbing components without failure is a much more severe threat than a larger obstacle which will involve more collision protection components.

Another key parameter in the design collision is the velocity with which the craft moves toward the obstacle. The collision energy E_{craft} which must be absorbed to stop the craft is defined by

$$E_{craft} = 1/2 MV^2 \quad (5)$$

where V is the collision velocity component in the direction of the obstacle, and M is the mass of the craft. Note that the energy is a function of the square of the velocity. It may be appropriate to define separate design collision velocities for separate regions on the craft. For example, higher velocity collisions are more likely on the bow than on the side peripheral structure.

Another point is that the most severe collision is such that the resultant of the crushing forces is directed toward the center of gravity (CG) of the craft. In other words, the collision is most severe if the obstacle contacts the craft dead center on the bow or on the side at the longitudinal location of the craft CG. A collision which occurs eccentric to the CG tends to rotate the craft horizontally. The effect is to reduce the effective craft mass since some of the translational energy which would have been directed at the obstacle is converted to rotational energy and is no longer involved in the collision. Of course, the resulting craft motions could easily result in a second collision at comparable or even higher velocity on a different region of the craft. Note that oblique impact (discussed earlier) and eccentric impact are not the same. Oblique impact is an impact at an angle other than 90 deg to the impacting craft surface. Since crushing force resultants are normal to the impacting surface, the oblique impact may or may not be an eccentric impact depending on its location on the craft.

When the kinetic energy of a 500-ton ASEV moving at 100 knots is compared with the collision protection potential, it is quickly seen that it is unreasonable to attempt protection for these conditions. Instead, a more reasonable collision design velocity should be defined, recognizing the necessity to reduce speed in high collision danger regions and to develop techniques and procedures for reducing the impact velocities when collision is unavoidable.

An evaluation of the energy-absorbing capability E_{cap} of a peripheral structure against a design collision is made with the following equation:

$$E_{cap} = \sum_{N_c} \int_{L_{eff}} F_c \, dx \quad (6)$$

where F_c is the crushing force of an individual collision protection component,

N_c is the number of components assumed to act in the design collision, and

L_{eff} is the effective component length.

If the energy-absorbing characteristics of the element are ideal, that is, if the crushing force is a constant through the effective element length, then Equation (6) reduces to

$$E_{cap} = N_c F_c L_{eff} \quad (7)$$

Since the design collision defines the collision velocity and since the mass of the vehicle is known, the design collision defines the required collision energy E_{req} . In an acceptable collision protection design, the energy-absorbing capability of the protection structure should equal or exceed the required collision energy. The design collision should also specify obstacle size which indirectly defines the number of components that would act in the collision. The component may therefore be designed by selecting a component crushing force and an effective length to satisfy Equation (8):

$$F_c L_{eff} \geq \frac{E_{req}}{N_c} \quad (8)$$

The ability of the primary structure to accept loads from the protection system without damage limits the value of the crushing load F_c . It is perhaps wise to impose some factor of safety on the crushing load to ensure no damage to the primary structure.

Since F_c and the required energy absorption per component are known, the effective length and therefore the real component length can be defined. The component is actually a configuration of energy-absorbing elements, however, and the crushing force in each element is defined by the configuration geometry. For a configuration such as that shown in Figure 12, the relationship between component and element crushing forces is:

$$F_c = N_e (\cos \alpha) F_e \quad (9)$$

where F_c is the crushing force of the component,

F_e is the crushing force of each element,

N_e is the number of elements per component, and

α is the angle between the elements and the axis of symmetry.

Individual elements may now be selected since the element lengths and the element crushing force are known. A closed form solution is:

$$1.0 = \frac{2\sigma_y L^2}{E(\pi R)^2} \left[0.911e^{-\frac{0.0523\pi^3 E R^4}{F_e L^2}} + 0.16 \right] \quad (10)$$

Equation (10) is derived from Equations (3), (4), and (5). Since it is desirable to ensure that Euler buckling does not occur, a factor of safety on the allowable length should be used: $L_{\text{allowable}} = (\text{F.S.}) \times L$.

However the closed form solution is difficult in that it involves the solution of Equation (10) for R. Instead, an iteration process may be used or the solution selected from tables prepared with the aid of the digital computer for a range of parameters and conditions.

Computer program COLIDE can be used to prepare parametric tables for a range of allowable element crushing forces. A description of the computer routine is presented later in this report. Appendix B is a sample of the output from this computer program for the case where the allowable element crushing force is 20 kip. The table is entered with the element length to obtain a design.

A study of the variance of the parameters of the table reveal a few interesting features. Note that as the ratio of R/t decreases, the energy-absorbing efficiency E/W rises but the total energy absorbed drops. This is a result of the influence of the cross-sectional parameters on the allowable element length to prevent fundamental Euler buckling.

It should be mentioned here that this technique is valid even for the cold Arctic environment. In fact, Morton and Silvergleit¹⁰ have shown that the properties of the most likely material, aluminum, are even better cold than at the ambient conditions of the impact tests. The prime material qualities are yield stress and elongation.

¹⁰ Morton, A. G. S. and M. Silvergleit, "Review of Candidate Structural Materials for an Arctic Surface Effect Vehicle," NSRDC Report 3573 (May 1972).

LOAD DISTRIBUTION SYSTEM

It is apparent from the specific energy-absorbing capabilities demonstrated earlier for major energy-absorbing components that more than one component must be involved in a collision in order to successfully halt a craft from any reasonable collision velocities. When the obstacle is large and appears to be infinitely wide to the craft approaching in a direction perpendicular to the surface of the ice, all obstacles on the contact side of the craft are automatically involved. In this case, all the energy-absorbing capability available in the collision direction is used.

It is anticipated, however, that reality will be somewhat different. It is more likely that the obstacle will be either irregularly shaped or smaller than the width of the craft, and the craft is likely to approach the obstacle at some angle other than 90 deg. Only a few of the energy-absorbing components will therefore be involved. The purpose of a load distribution system (see Figure 16) is to span the major energy-absorbing components and distribute the loading to those which would otherwise not be involved. Naturally, if more energy-absorbing structure is involved, higher craft velocities can be tolerated in a collision.

It is obvious that a load distribution system is necessary when the major energy-absorbing components are discrete units such as tube configurations. The system is necessary here to provide collision protection when the ice obstacle impinges on the craft extremity between two components. Without the distribution system, the collision impact would be felt directly on the structure to be protected and damage would occur. In the case of a continuous major component such as the air bag, the distribution system may be used to involve more of the air bag in the energy-absorbing process.

The load distribution system must be designed to elastically distribute the design loading to a specified number of additional components. The system would then be allowed to form plastic hinges at the edges of the involved extremity structure and at the edges of the obstacle contact region.

As the collision progresses, the major energy-absorbing components within the obstacle contact region would gradually collapse, absorbing energy. The load distribution system would distribute the impact load to

components that would not otherwise have felt the loading, causing these components to collapse, absorbing additional energy. If sufficient energy could not be absorbed within the elastic range of the distribution system, the system would form plastic hinges, absorbing additional energy itself and allowing the major energy-absorbing components to collapse further.

Since it cannot be predicted where a collision will occur along the extremity structure, the load distribution system must be continuous along a given side of the craft. It may be desirable to provide discontinuity at the "corners" of the craft to prevent excessive loading transverse to the major components, for example, along the side as a result of a bow collision.

The load distribution system is analyzed as a continuous beam on rigid foundations (the components). The analysis must be done incrementally in displacement between the displacement when a given number of major components are collapsing to the displacement when one or more additional components begin collapsing. The problem was solved by using the three-moment equations¹¹ for the case where the obstacle delivers a concentrated load. When the load is at center span between two major components, the moment in the beam at the first noncollapsing major component is defined by:

$$M_e = \frac{4K_{ed}}{24N + 19} \quad (11)$$

Here M_e is the moment at the first noncollapsing component, N is the number of components plastically collapsing on either side of the impact load (while the beam is completely elastic), and K_{ed} is defined as:

¹¹Borg, S. F. and J. J. Gennaro, "Advanced Structural Analysis," D. Van Nostrand Company, Inc., New York, New York (1959), pp. 80-83.

$$K_{ed} = \frac{-3 P \ell}{2} \left[\frac{1}{4} + 2 \sum_{m=1}^N m \right] - 3 F_c \ell \left[2 \sum_{m=1}^{N-1} (N - m) (m) \right. \\ \left. - 2 N_c \sum_{m=1}^N m \right] \quad (12)$$

where P is the impact load,

ℓ is the span length between components, and

F_c is the plastic collapse load of the energy-absorbing components.

The load on the first nondeforming component R_e is defined as:

$$R_e = \frac{-5 K_{ed}}{\ell (24 N + 19)} + P/2 - N F_c \quad (13)$$

Note that when N is chosen, the span length ℓ is known, and the system is designed for a value of F_c , Equations (12) and (13) become two simultaneous equations in P and K_{ed} .

When they are solved, the results may be used in Equation (11) to determine M_e . The following equation defines the shear at the extremity of the collapse region V_e :

$$V_e = P/2 - N F_c \quad (14)$$

The moment and shear diagrams for the load distribution system in the collapse region may now be defined. Although the moment at the point of the loading is usually maximum, other points in the system may have higher moments than that defined at the extremity of the region in equation (11). Therefore plastic hinges may form at unexpected locations. Figure 17 presents the shear and moment diagrams for two loading conditions. Loading Condition A is the case where the total number of components allowed to collapse is four (i.e., $N = 2$); Case B is the case where the total number of collapsing components is six (i.e., $N = 3$). The value chosen for F_c is 25 kip. No inferences as to typical craft capabilities should be drawn from this assumed value since its selection was completely arbitrary.

Figures 18 and 19 show the collapse mode of the load distribution system where $N = 2$ for the cases where the obstacle contact is between major components and directly on a major component, respectively. Note that none of the major components collapses completely. If plastic hinges form, as shown in the distribution beam, then the total impact load and energy-absorbing capability are calculated as follows:

$$P = F_c \sum_{m=1}^{2k} x_m + \frac{4 M_p \theta}{L_{eff}} \quad (15)$$

and

$$E_{cap} = P L_{eff} \quad (16)$$

where P is the impact load,

x_m is the maximum crush distance for the m^{th} component,

M_p is the plastic moment capability of the distribution beam,

θ is the angle of plastic rotation of each plastic hinge,

L_{eff} is the maximum crush distance for the major components under the loads or the component depth, and

E_{cap} is the energy-absorption capability.

Note that the numerator of the second term of Equation (15) is the energy contribution by the distribution beam.

The parameter k is the number of components on either side of the load which will collapse plastically after the formation of the plastic hinge at the point of load. This must be determined by analyzing the system illustrated for increasing values of k until the beam exhibits a second plastic hinge. The value of k is then defined as the value which first causes a second plastic hinge to form in the distribution beam.

In order to determine the location of the second or outer plastic hinges, it is necessary to determine where in the distribution beam the second highest moment peak exists. Since this location is next in line to reach the elastic limit, the plastic hinge will next form at that location. It is seen from the moment diagrams of Figure 17 that for a distribution beam strong enough to span two or more collapsing components before the formation of the initial plastic hinge, the second hinge will form at

the third major component from the point of load. Since for somewhat stronger beams, the second hinge will continue to form at this same point, it is not greatly advantageous to require greater strengths for the distribution beam than that necessary to span two collapsing components external to the load point. Additional energy is gained in the rotation of the beam when the plastic moment is increased, but no additional major energy-absorbing components are added for a range of beam strengths. Since energy is absorbed much more efficiently in the major components than in the distribution beam, it is more advantageous to design the beam for the lower end of this strength range.

It may be necessary to investigate the situation beyond the beam strength range discussed above if sufficient energy cannot be absorbed within the involved collision area of this beam strength. For the present, however, it will be assumed that two components on each side of the impact load area will collapse and therefore that k has a value of two.

All of the relationships presented here are derived for the case where the load is concentrated at center span. Since this can be shown to be the worst-case loading, it is therefore chosen as the design loading. If the impact load actually occurs at a different location, such as directly over a major component, the system will have somewhat more capability than in the design situation.

Although the preceding discussion has been for the case where the impact load was a concentrated load, the theory is easily extended to a distributed impact load in the following manner. The distribution system is treated as if the entire obstacle contact area were displaced as a unit, allowing no internal shear or rotation. All components within the contact area may therefore be totally crushed. The distribution system is designed as though the load were concentrated at the boundary of the obstacle contact area. The plastic hinges form there and at the first noncollapsing major components (see Figure 20).

When the load distribution system is designed, an additional factor must be taken into consideration. The system must be designed so that the impact load does not cause local collapse of the distribution beam in the obstacle contact area, resulting in premature formation of the initial plastic hinge in this area. Not only would the plastic moment be

considerably lower, but also the beam would then not be capable of distributing the collision load to additional major energy-absorbing components as effectively.

STEPS IN THE DESIGN PROCEDURE

The design procedure then is as follows:

1. Based on the craft motions and the ice obstacle size, define a design collision for each area of the craft to be protected.

2. Define the number of energy-absorbing components which will act in the design collision.

3. Define the limit load which the collision protection elements can apply to the primary craft structure without causing damage. Divide this limit load by an appropriate factor of safety to ensure no damage.

This defines the element crush load F_e .

4. Calculate the kinetic energy of the moving craft at the time of the collision (Equation (5)).

5. Calculate the energy which must be absorbed per energy-absorbing element to fully absorb the kinetic energy of the craft at collision:

$$E_e = E_{craft} / N_c N_e \quad (17)$$

where E_e is the energy absorbed per element,

E_{craft} is the kinetic energy of the craft at collision,

N_c is the number of components assumed to act in the design collision, and

N_e is the number of elements per component.

6. Determine the geometric efficiency factor G for the configuration based on the usable length of the configuration in the crushing process.

The geometric efficiency factor essentially relates the component length to the length over which the component effectively absorbs energy:

$$G = \frac{L_{eff}}{L_c} \quad (18)$$

7. Calculate the element length required to absorb the energy per element E_e , calculated in Equation (5):

$$L_e = \frac{E_e}{F_e G (\cos \alpha)^2} \quad (19)$$

8. Enter the tables produced by computer routine COLIDE with the element length L_e and the element crushing force F_e and extract the cross-sectional dimensions of the energy-absorbing element.

COMPUTER PROGRAM COLIDE

A computer routine has been written to calculate the crushing characteristics of thin-wall extruded tubing in the inextensional buckling mode. The routine is called COLIDE and is operational on the CDC 6700 digital computer system located at NSRDC.

The input to the program includes the limit load or the crushing force of the tube element, the orientation of the tube in a component, material properties, and the efficiency factor for the configuration geometry. The output provides the optimum length of the tube element, the tube cross-sectional properties, and the energy-absorbing capability for the tube element in the configuration. The program was written to allow a parametric study of the critical properties of the tube in an energy-absorbing role. The output of the routine in tabular form is useful as a design tool.

The input to the program is by cards which must be prepared in the following format.

CARD 1: (Format 6A10) - BTITLE - a title for the problem. This title will be used to label all printed output.

CARD 2: (Format 6F10.2) - FPLOW, FPHIGH, FPINC

FPLOW - the minimum value of the allowable crushing force (in kip) for each tube element.

FPHIGH - the maximum value of the allowable crushing force (in kip) for each tube element.

FPINC - the increment of the allowable crushing force (in kip).

This card defines the range of allowable crushing forces to be considered and the incremental variations of the crushing force. A table of all the tube designs and characteristics will be output for each crushing force.

CARD 3: (Format 6F10.2) - XKMIN, XKMAX, XKINC

XKMIN - the minimum value for the energy factor or the cross-sectional efficiency K.

XKMAX - the maximum value for the energy factor or the cross-sectional efficiency K.

XKINC - the increment of the energy factor. A series of tube cross sections will be designed, ranging from a minimum to a maximum energy factor at each increment XKINC for each crushing force defined on the previous card.

CARD 4: (Format 6F10.2, I10) - SIGMA, ANGLE, FACSF, EFFGMY, EMOD, DENSE, NE

SIGMA - the yield stress of the tube material (in ksi).

ANGLE - the orientation angle of the element with respect to the axis of symmetry of the configuration (in degrees).

FACSF - the factor of safety against fundamental buckling.

EFFGMY - the geometric efficiency factor for the component configuration. This value relates the effective length of the component to the full component length.

EMOD - the elastic modulus for the tube material (in ksi).

DENSE - the density of the tube material (in lb/in³)

NE - the number of elements in a component.

Appendix B shows a sample of the output. The program listing is presented in Appendix C.

EXAMPLES

A few designs were evaluated in order to describe the collision protection potential and the associated weight penalty. In one case the design collision chosen was the 20-knot collision of a 500-ton ASEV. The collision was assumed to be head on and with an obstacle sufficiently large to involve all the components of the bow protection system (15 components). An element crushing force of 60 kip was assumed and a geometric efficiency

factor of 2/3 was used. A factor of safety against the buckling load was taken as 2.0. The design for this case is a tube with a 2.7-in. radius and a wall thickness of 0.177 in. Each element is 7.84 ft long and weighs 28.6 lb. The total weight of the bow protection system for the collision is thus 1715 lb. This does not include the load distribution system.

Another case evaluated was for the same collision conditions and the same size craft, but for an element crushing force of 30 kip. For this design, the tube radius was 3.96 in., the wall thickness 0.113 in., and the length 15.7 ft. The weight of the total bow protection system was 3214 lb.

These samples are presented to illustrate the kind of weight penalty included in collision protection for relatively low velocities. Since the weight will increase approximately as the square of the collision velocity, the penalty will be much more severe in the range of cruise velocities proposed for the ASEV. It is evident, then, that it is not feasible to protect against collisions at that velocity. It is also apparent that the collision protection weight penalty is heavily dependent on the allowable crushing force of the element. If the craft primary structure is capable of accepting higher loads from the elements of the collision protection system, the weight penalty will be lower. Figure 21 presents the weight penalty as a function of design collision velocity for the bow only, assuming a constant number of involved energy-absorbing elements. These data do not include weight in the load distribution or low energy bumper systems.

SUMMARY

The test data show that the energy-absorbing characteristics of the thin-wall extruded tube in inextensional buckling are nearly ideal. In other words, the crushing force is very nearly constant throughout the collision.

A design method is presented for peripheral collision protection structure in general and specifically for the thin-wall tube elements. A means of calculating the response of a load distribution system is presented. Test data are documented, and empirical relationships are derived for several energy-absorbing elements. A computer routine has been developed to produce in tabular form the variation in the energy-absorbing

characteristics of a tube in inextensional buckling with various cross-sectional parameters of the tube. The tables produced by such a program are a useful design tool.

The collision protection philosophy is summarized basically as follows. Ideally, the crushing force should be a constant and should not vary with velocity. It should be as high as possible for most efficient energy absorption and yet be less than the force which would cause damage to the craft primary structure. The energy absorbed by the elements of the protection structure must balance the kinetic energy of the craft in the direction of the collision obstacle or the obstacle will contact and damage the craft primary structure and probably other vital systems in the immediate area.

The definition of a design condition for collision must be based on the ability of the ASEV to avoid an obstacle, the probability of dangerous obstacle contact in a given region, the operational speeds in a dangerous region, and the ability of the craft to reduce speed before colliding with a detected obstacle. The amount of collision protection structure to be included must be defined for the design collision on the basis of the size and strength of the obstacle and the design of the load distribution system.

In the few design examples of collision protection systems for the bow of a 500-ton ASEV, the obstacle was assumed to be large enough to affect the whole bow. The total weight of the protection (excluding the load distribution system) for an element crushing force of 60 kip was about 1715 lb for a 20-knot collision.

Under the same conditions but for an element crushing force of 30 kip, the weight is predicted to be about 3214 lb. These weights indicate that protection for collisions of this order are feasible if the element crushing forces can be tolerated by the craft primary structure.

ACKNOWLEDGMENT

Much of the experimental work which led to the design methods and empirical relationships presented here was accomplished with the valuable aid of William R. Conley, NSRDC Code 1745. Mr. Conley also conducted the study of the crushing characteristics of cylindrical tubes as low velocity bumpers.

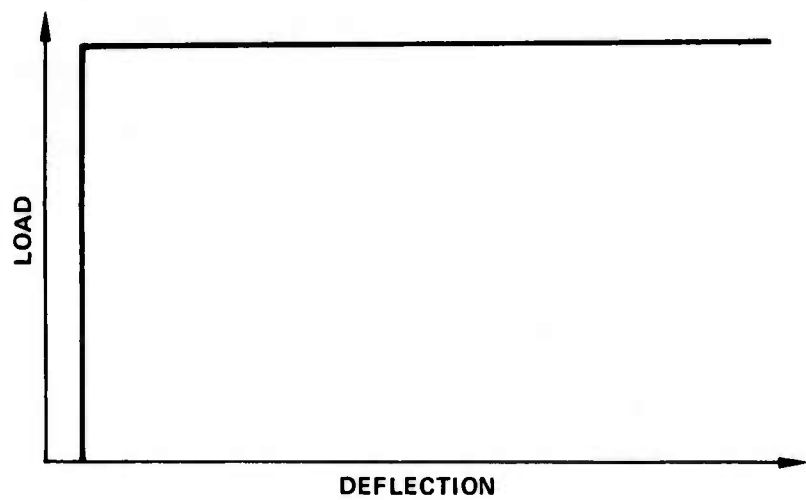


Figure 1 - Ideal Load Deflection Curve for Energy Absorption

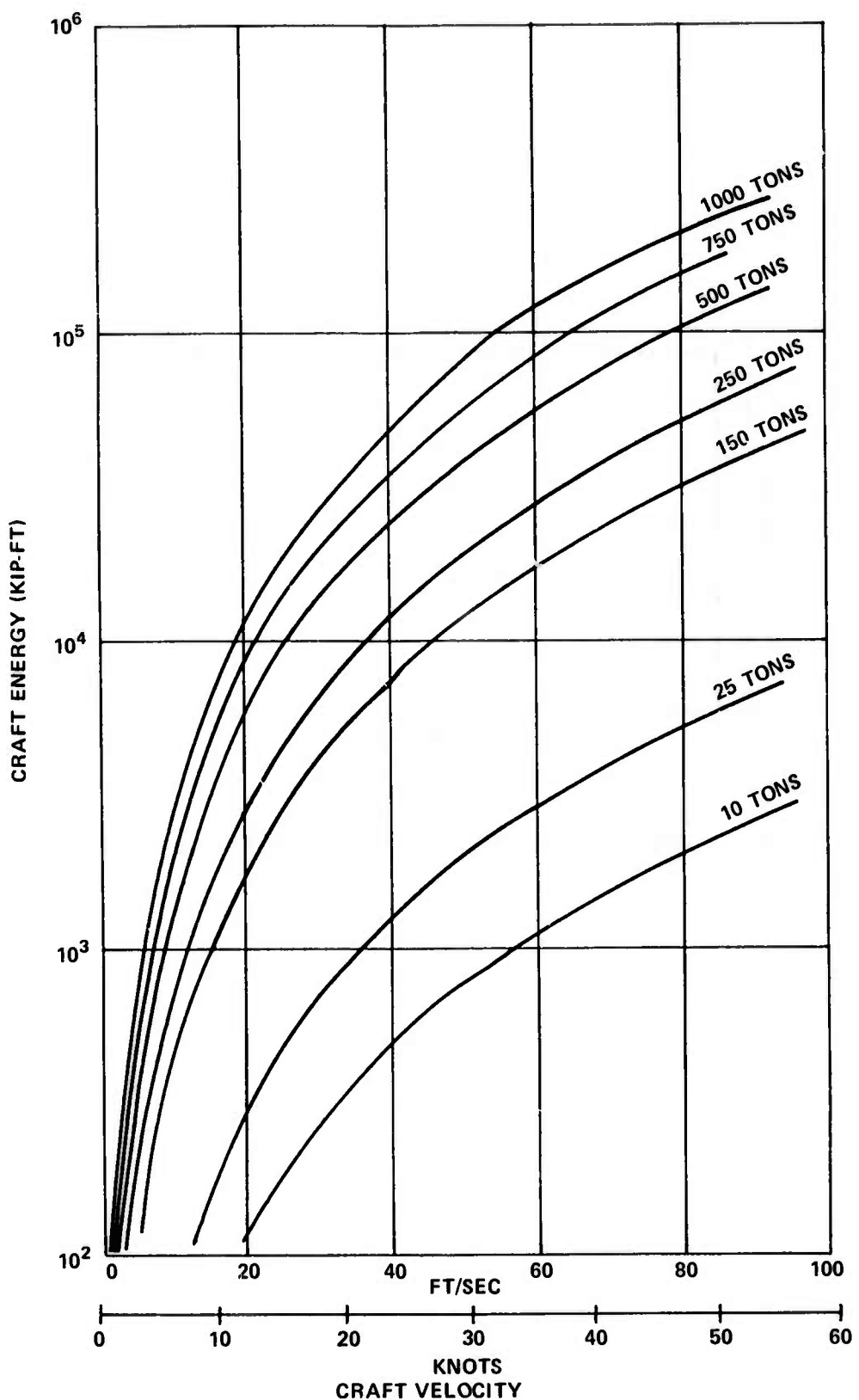


Figure 2 - Kinetic Energy versus Craft Velocity

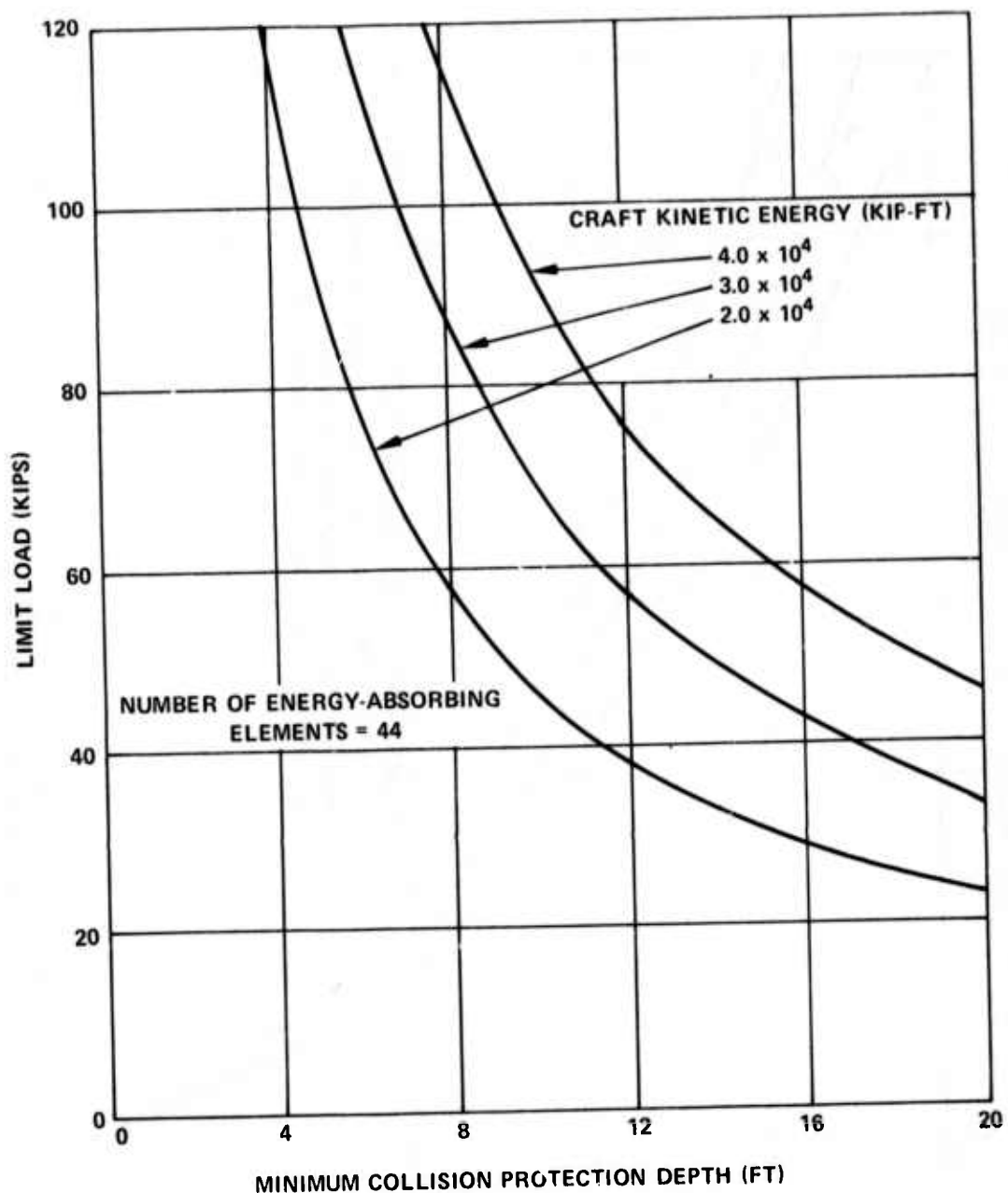
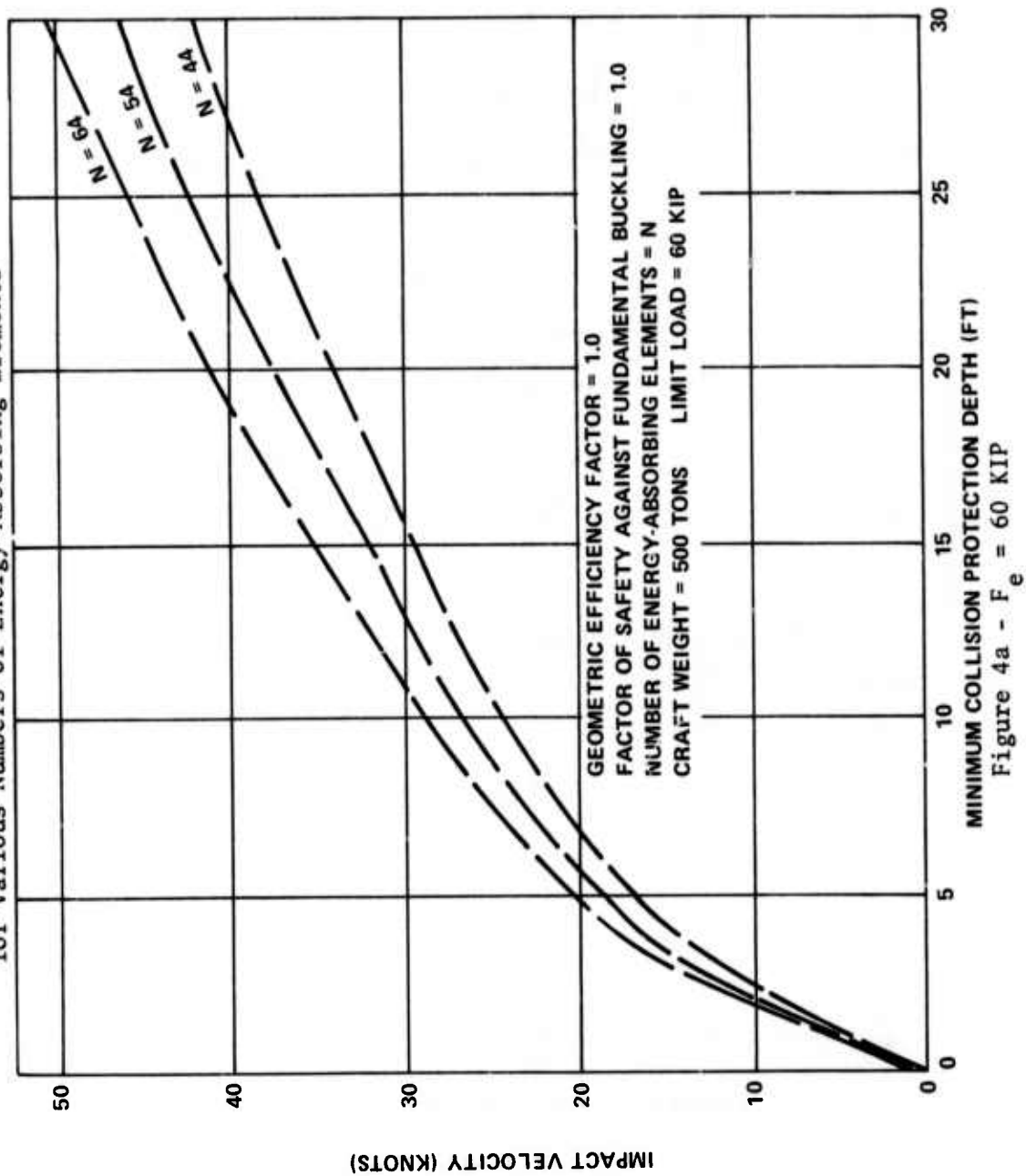


Figure 3 - Minimum Collision Protection Depth versus Limit Load for Various Craft Kinetic Energies

Figure 4 - Minimum Collision Protection Depth versus Impact Velocity
for Various Numbers of Energy-Absorbing Elements



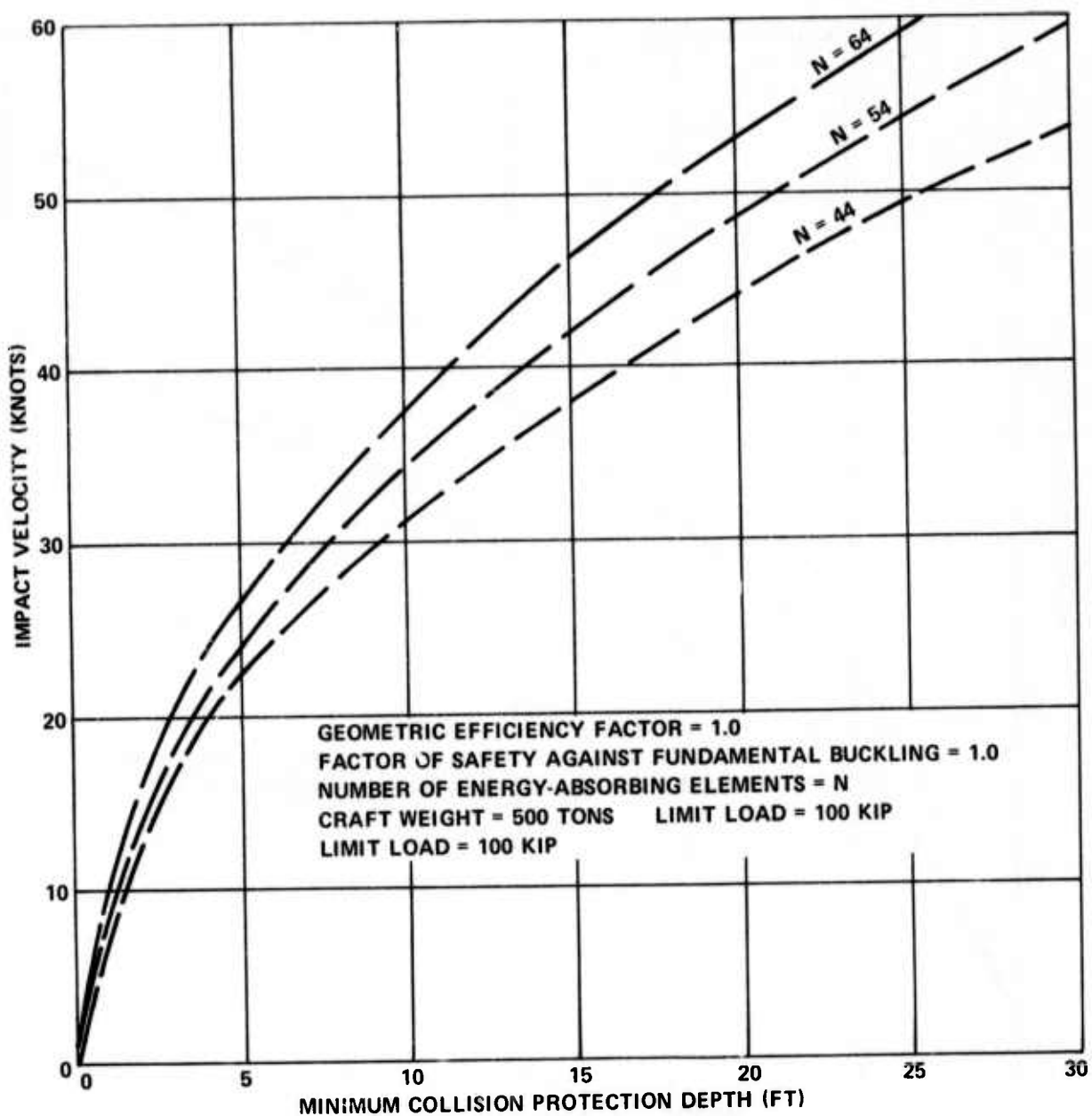


Figure 4b - $F_e = 100$ KIP

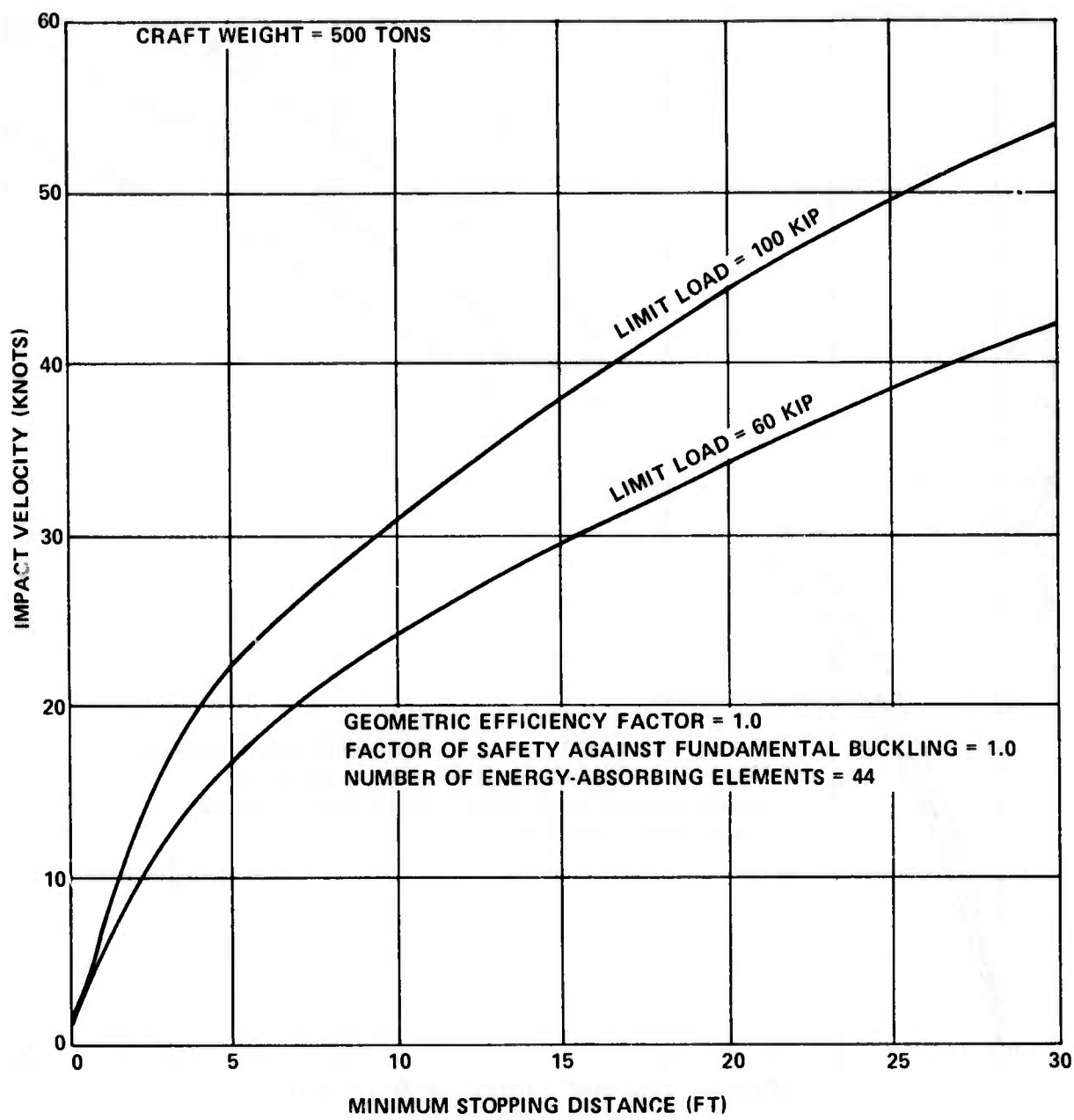


Figure 5 - Minimum Stopping Distance versus Impact Velocity for Various Limit Loads

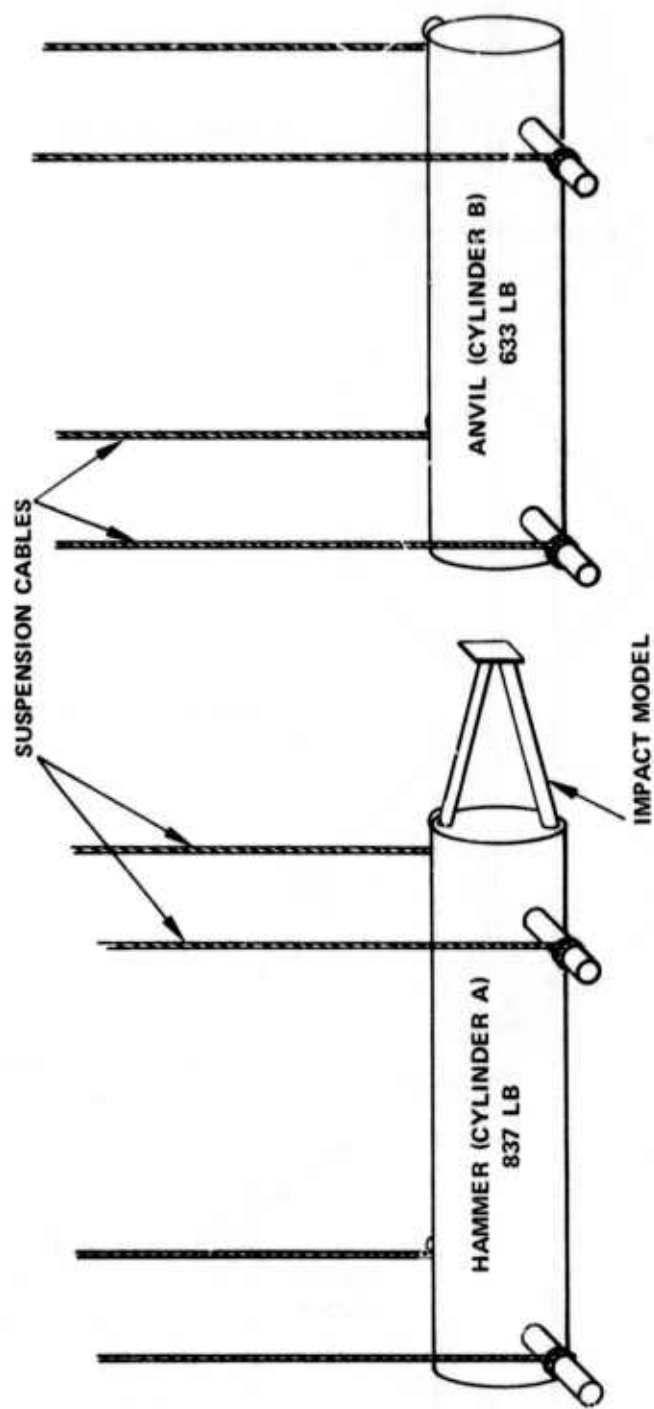


Figure 6 - NSRDC Ballistic Pendulum Facility

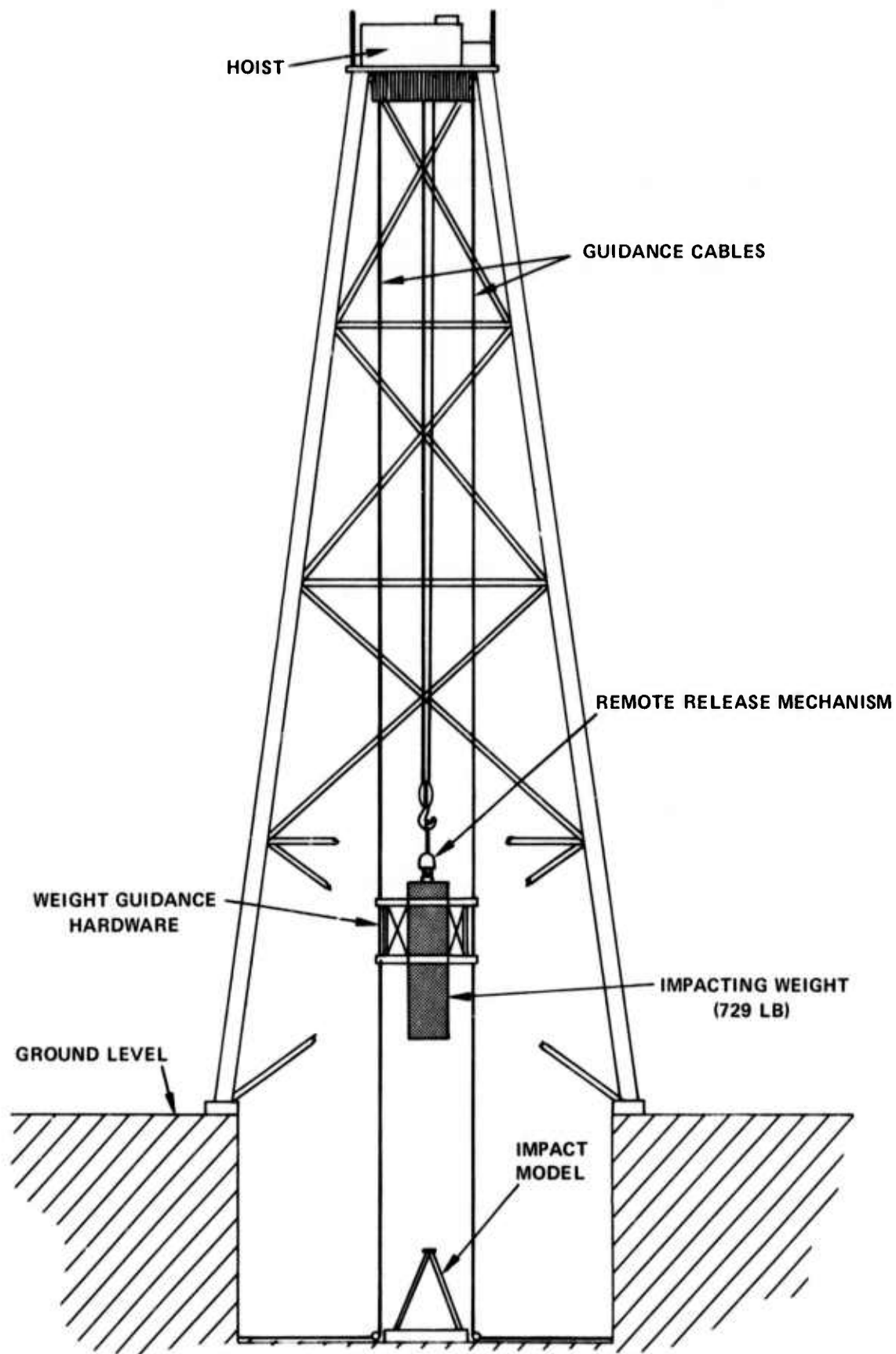


Figure 7 - NSRDC Drop Tower Facility

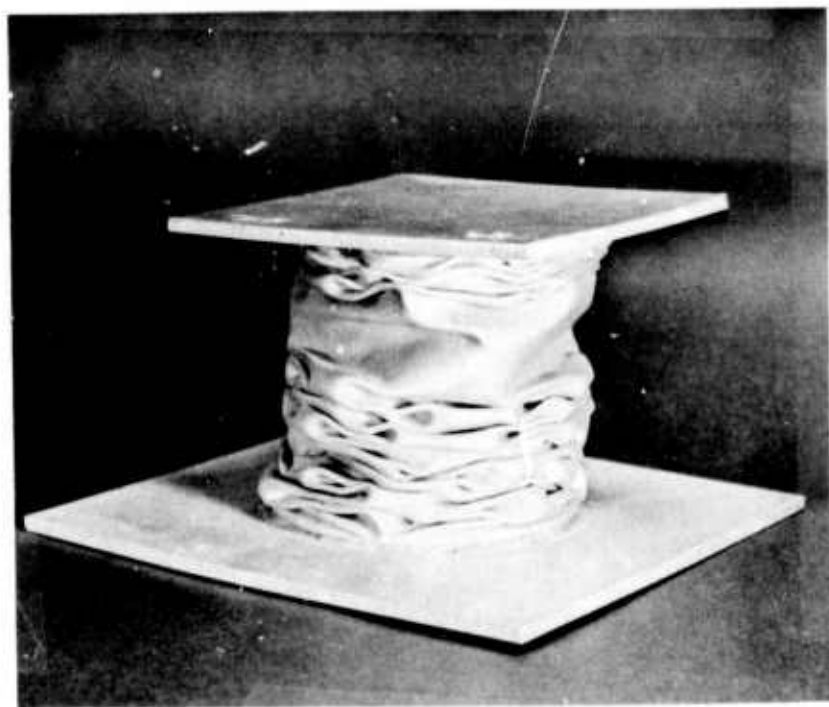
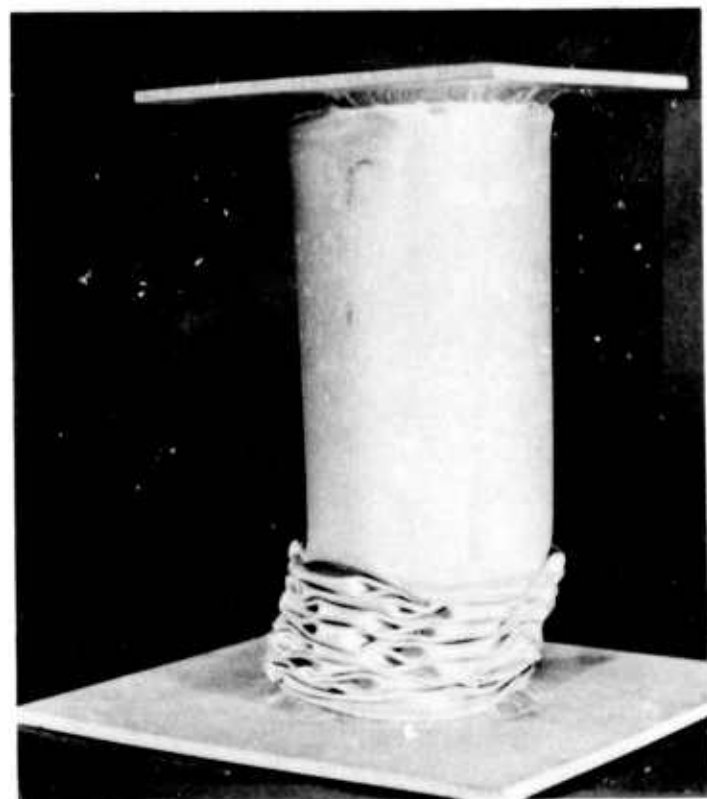


Figure 8 - Inextensional Buckling in a Thin-Wall Cylindrical Tube



Figure 9 - Component Configuration with Two Energy-Absorbing Elements

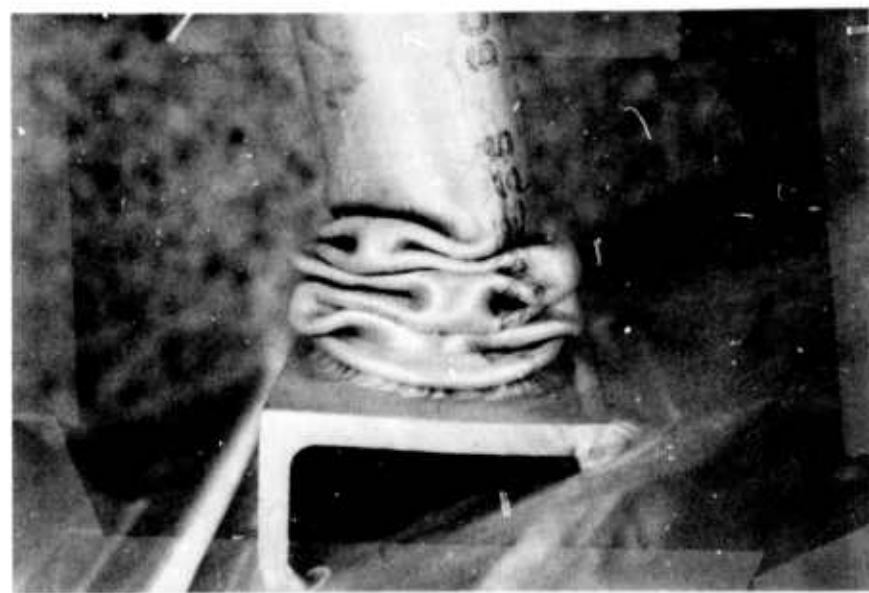


Figure 10 - Base Support Modification for Multielement Configurations

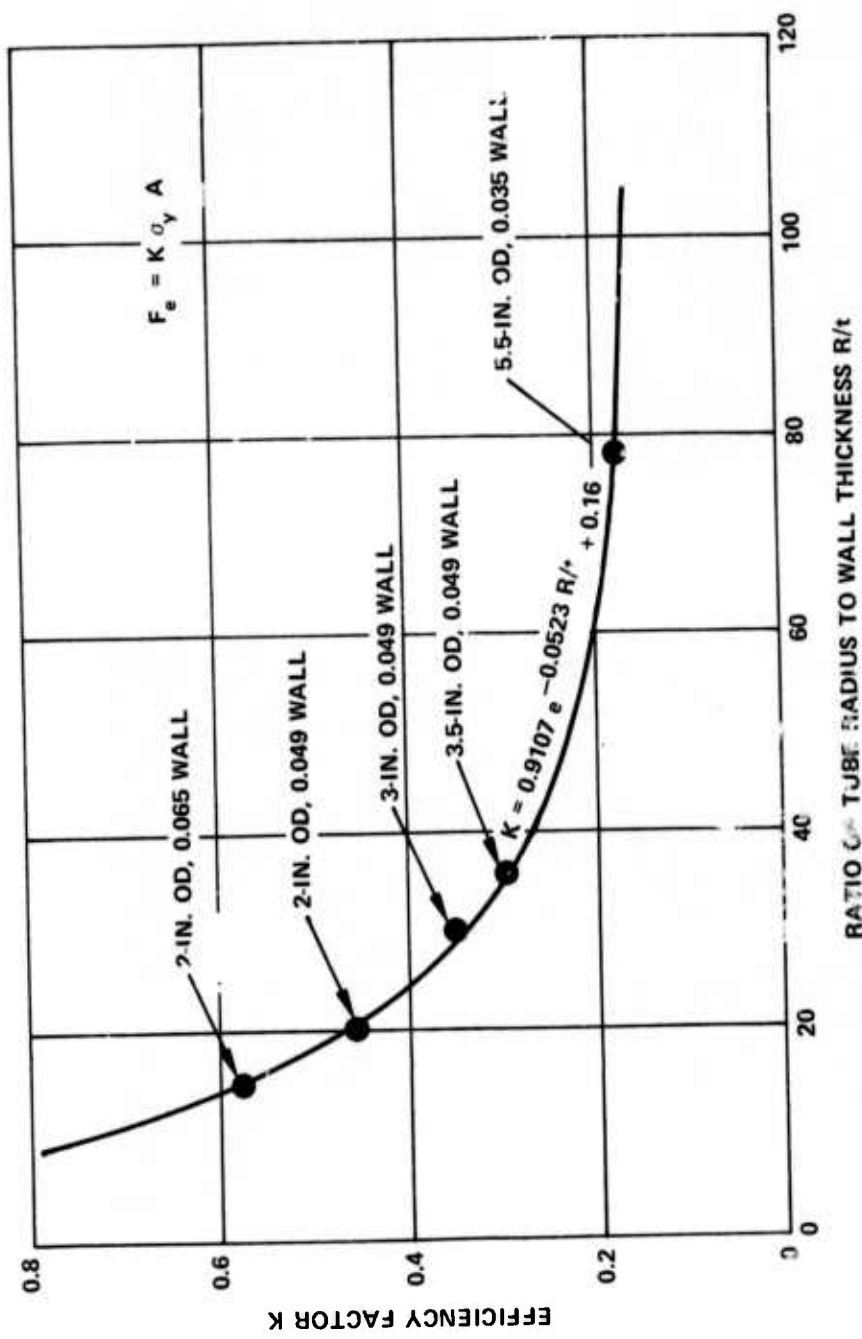


Figure 11 - Experimentally Determined Efficiency Factors for the Tube in Tensional Buckling

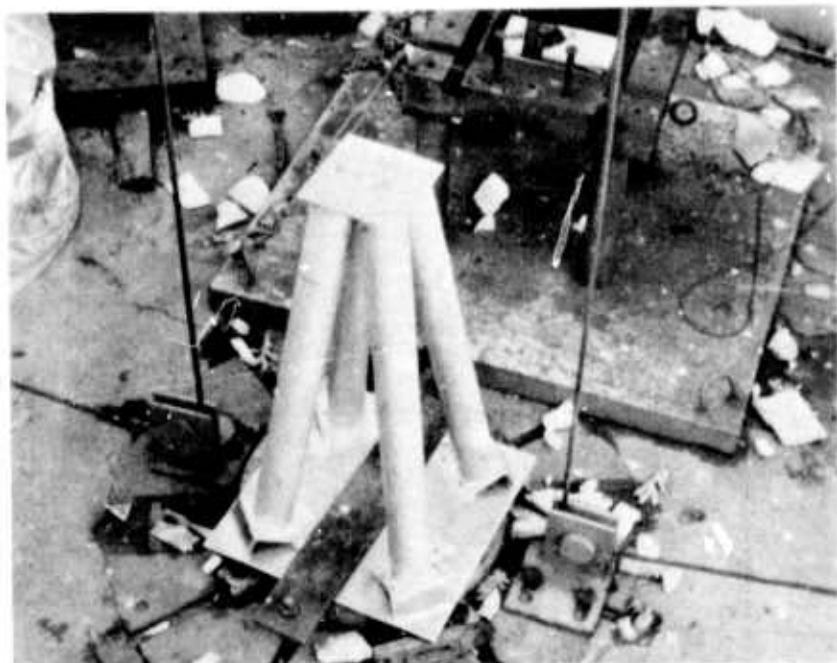


Figure 12 - Component Configuration with Four Energy-Absorbing Elements

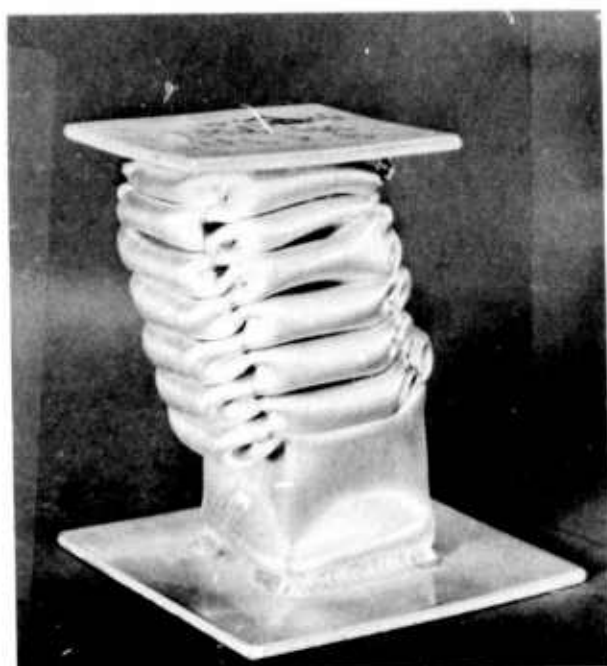
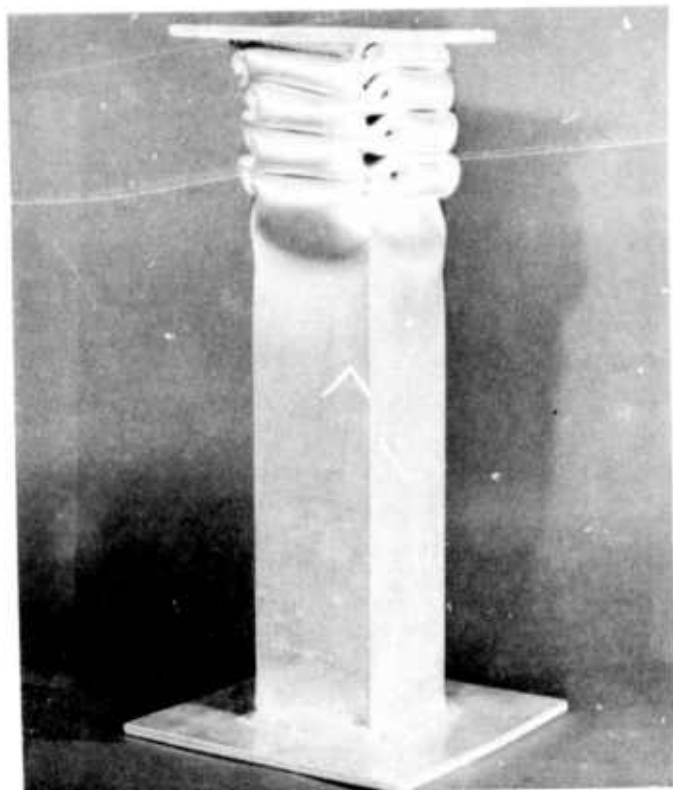


Figure 13 - Inextensional Buckling in a Square Tube

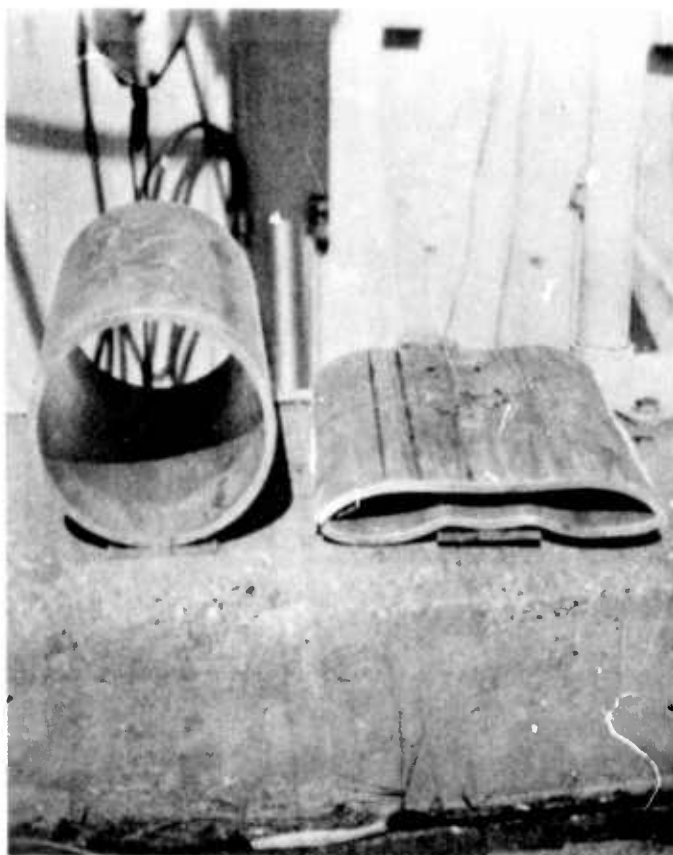


Figure 14 - Typical Bumper Tube Collapse

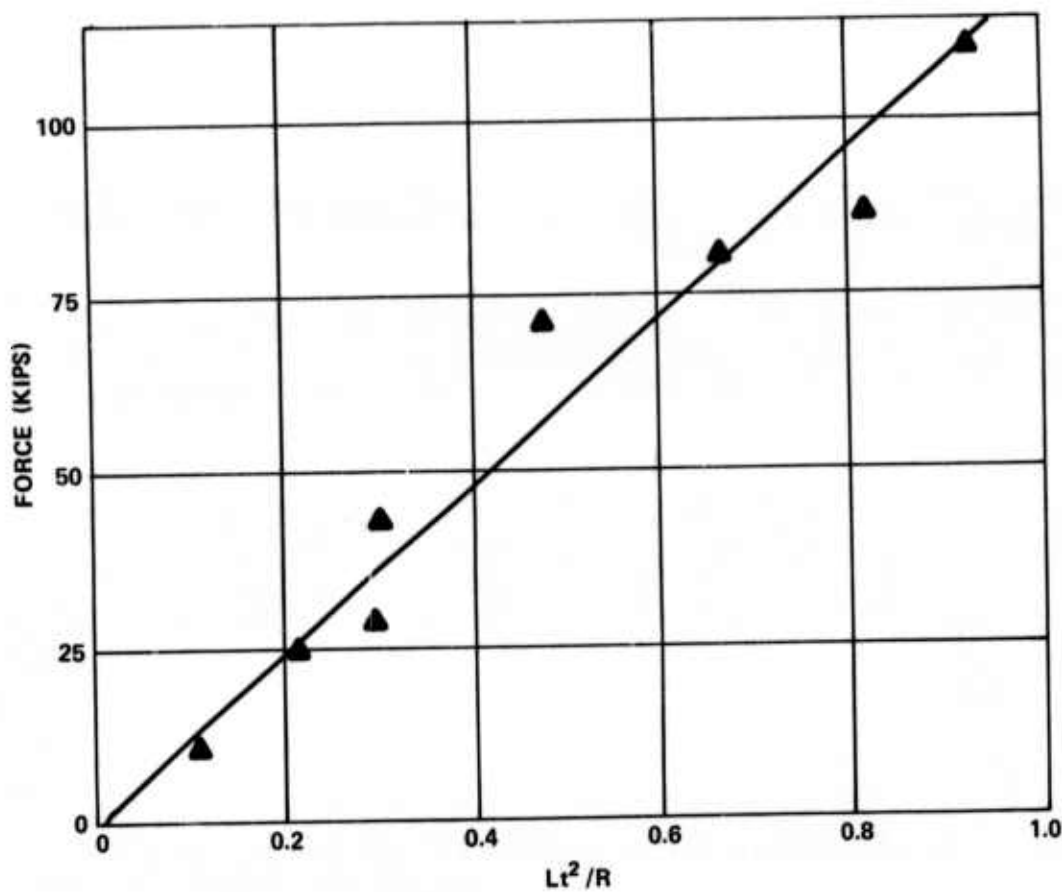


Figure 15 - Crushing Force of the Cylindrical Tube as a Bumper

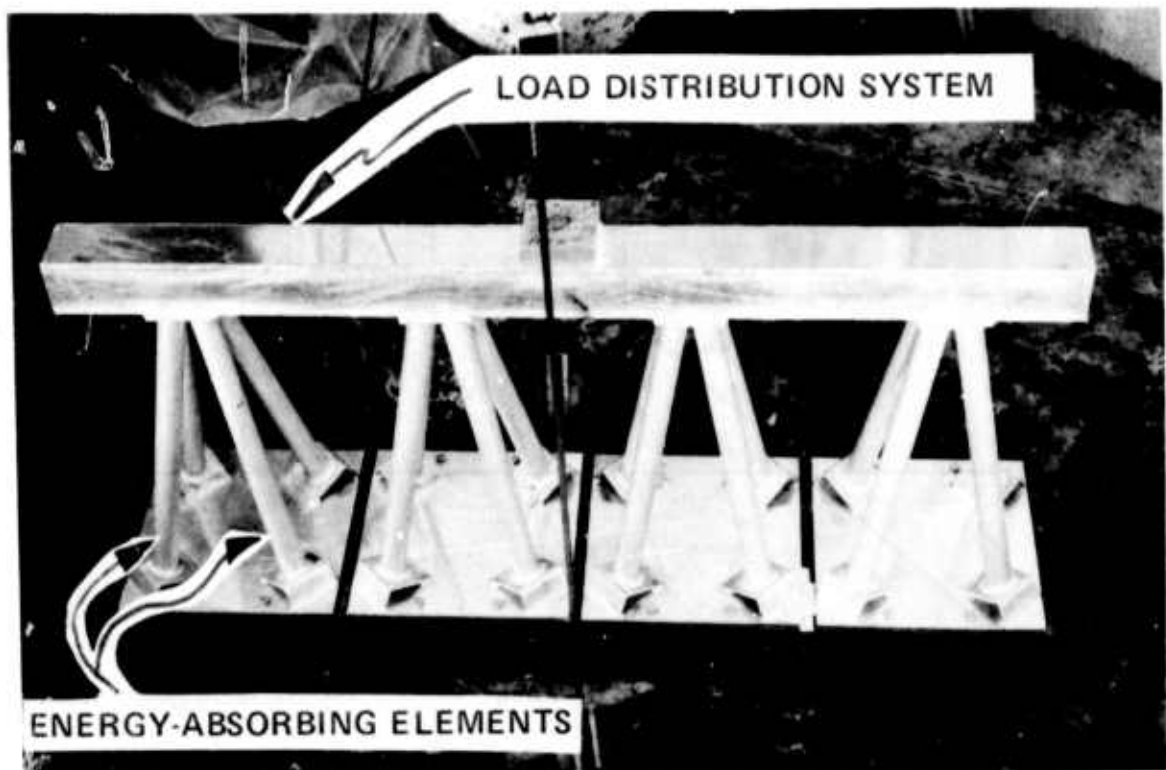


Figure 16 - Location of the Load Distribution System

Figure 17 - Shear and Moment Diagrams for the Load Distribution System

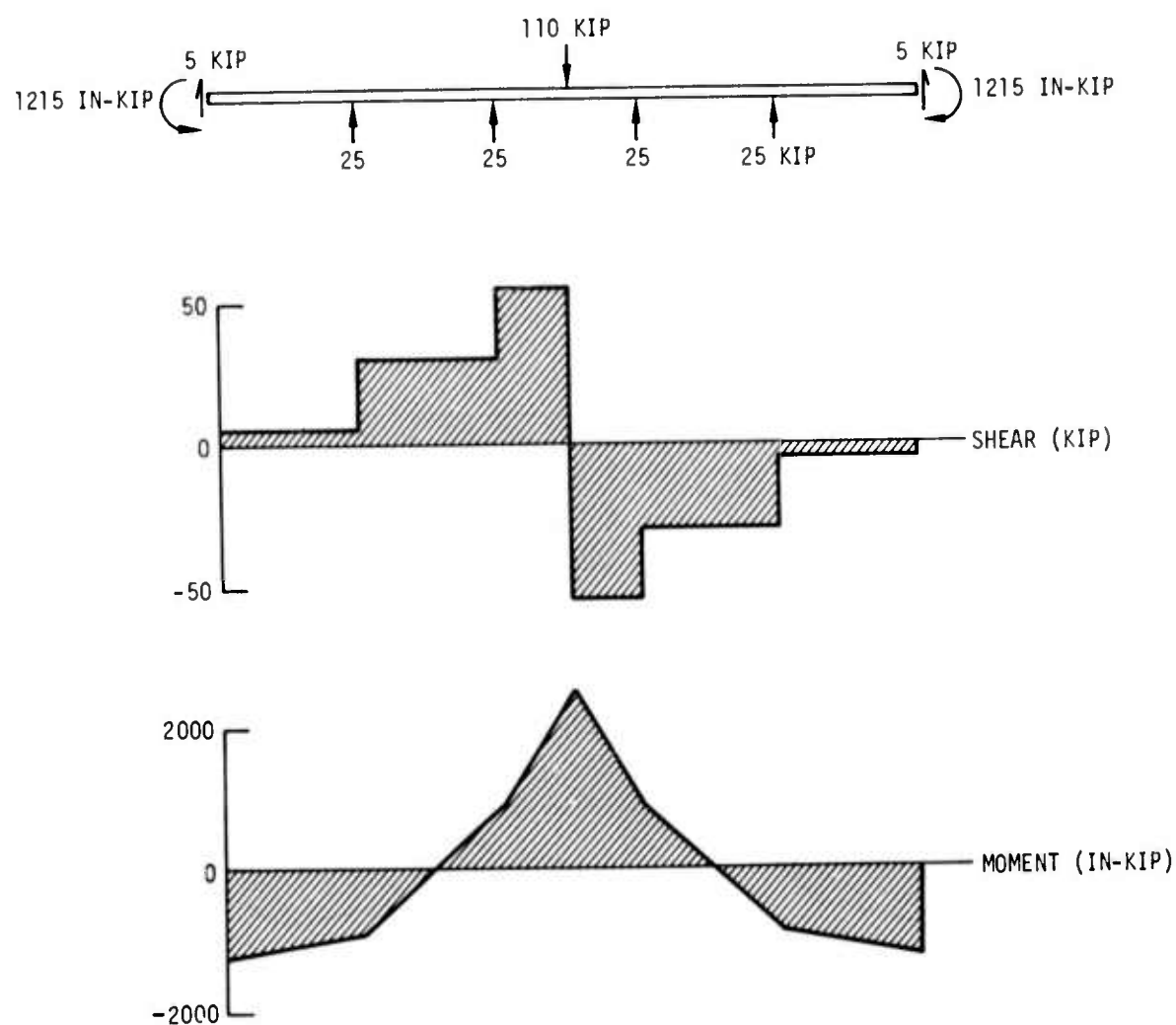


Figure 17a - With Four Crushing Components

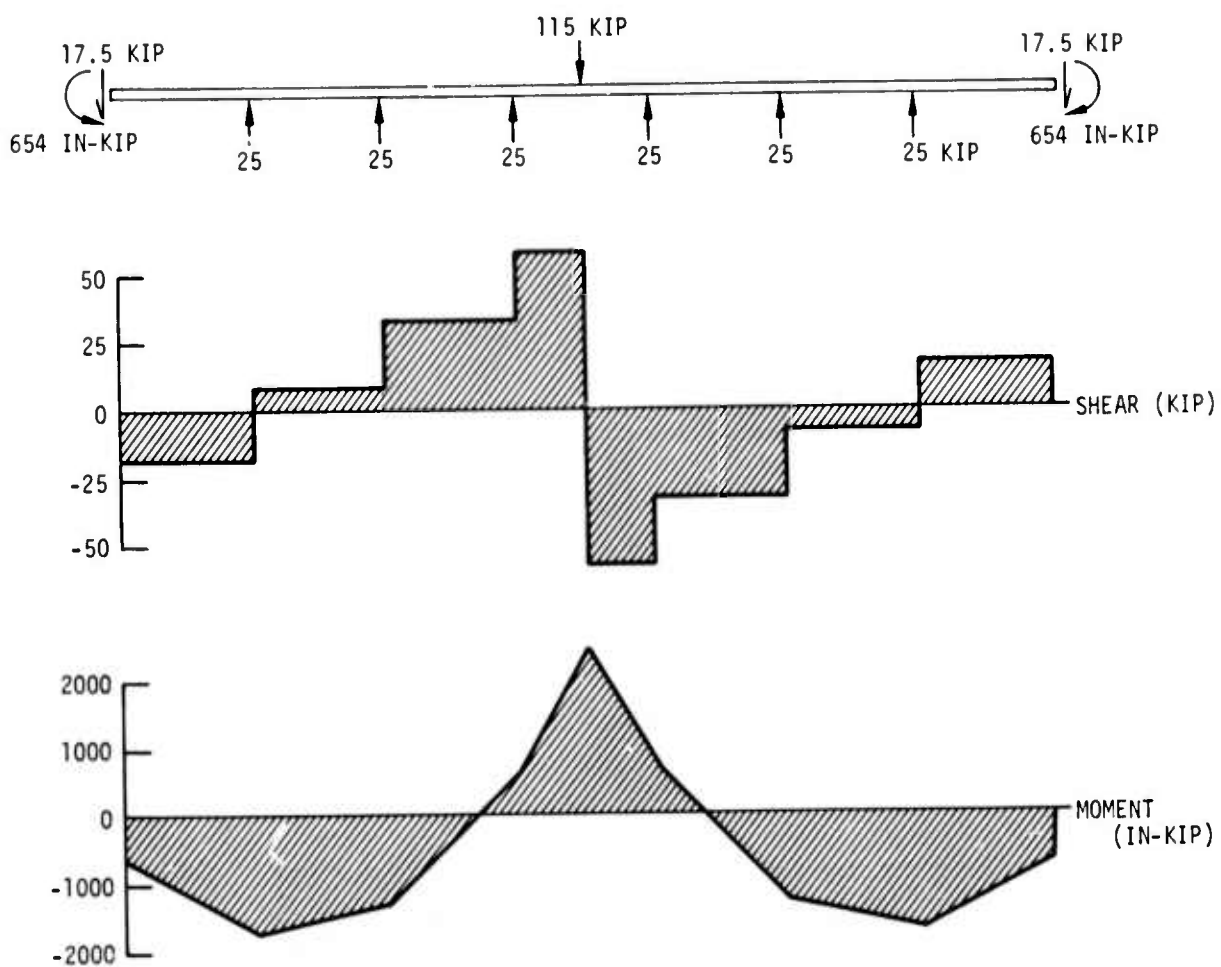


Figure 17b - With Six Crushing Components

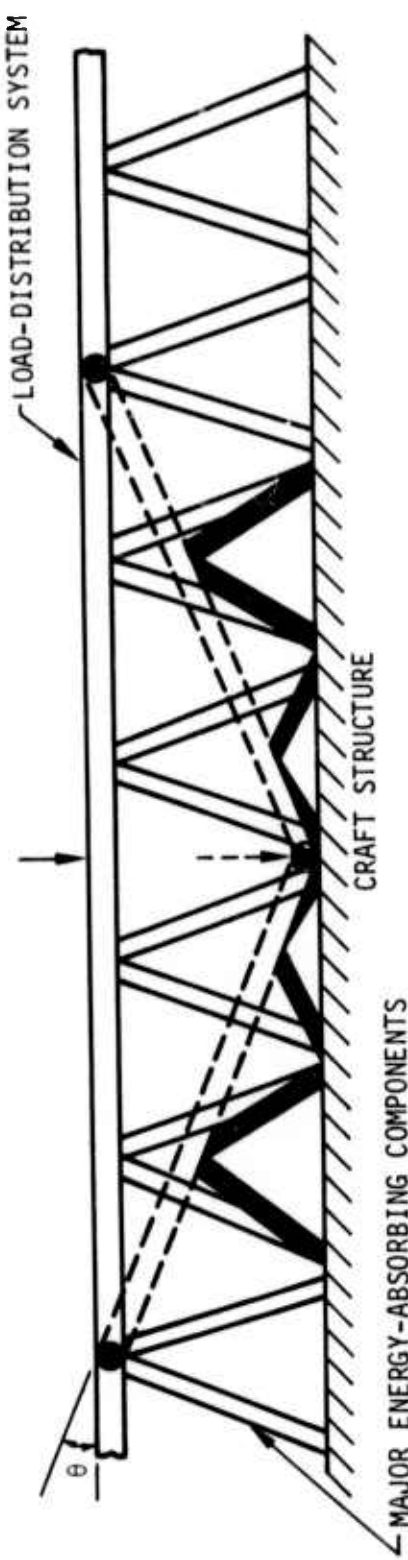


Figure 18 - Collapse of the Load Distribution System with Obstacle Contact between Energy-Absorbing Components

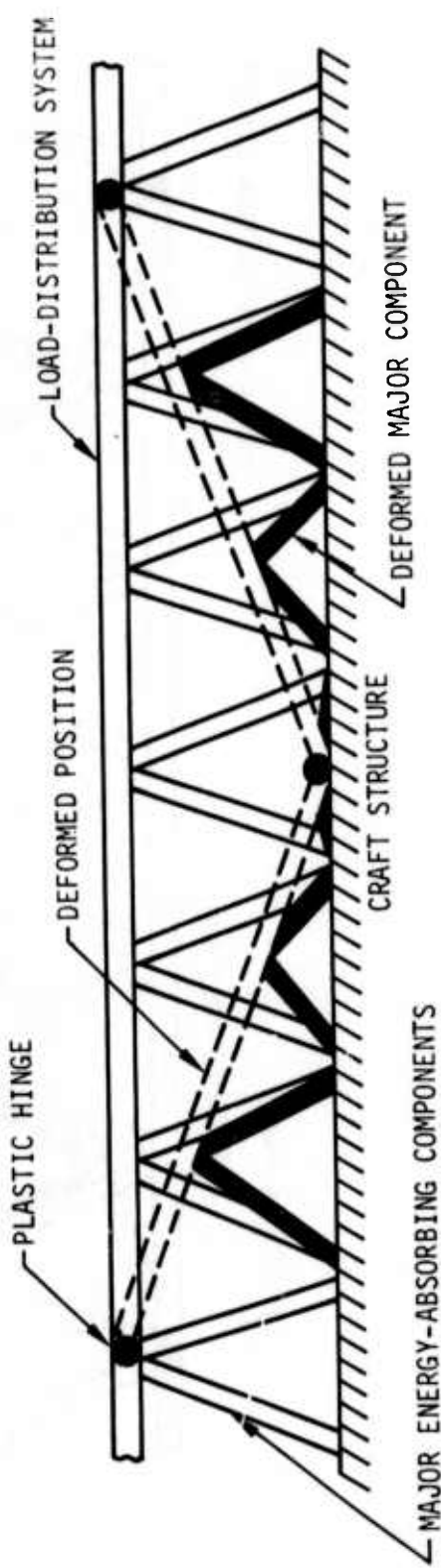


Figure 19 - Collapse of the Load Distribution System with Obstacle Contact on an Energy-Absorbing Component

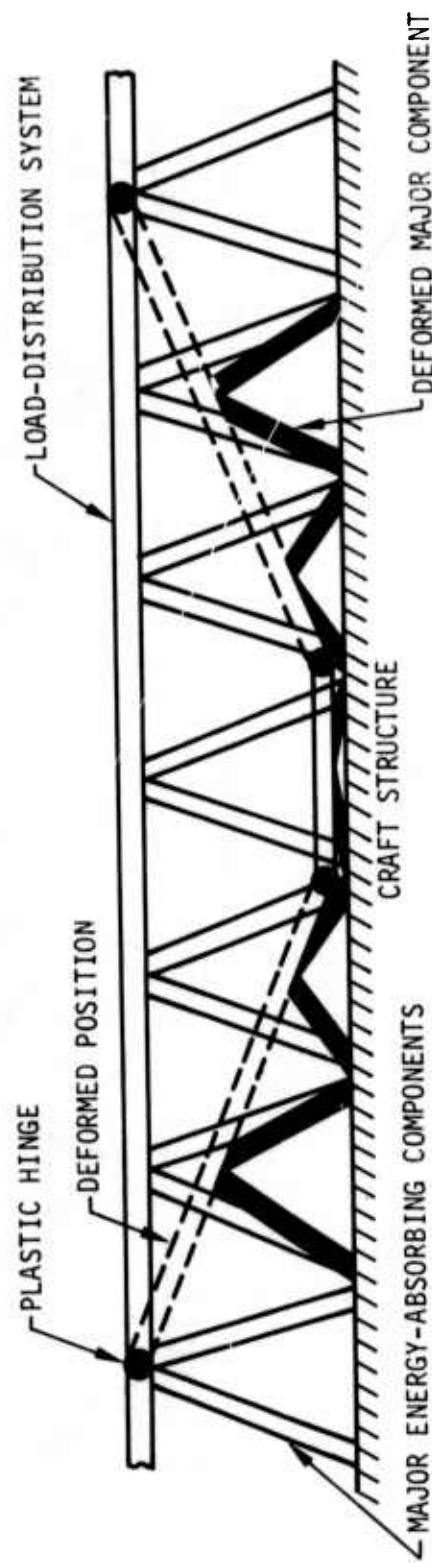


Figure 20 - Collapse of the Load Distribution System under a Finite Sized Obstacle

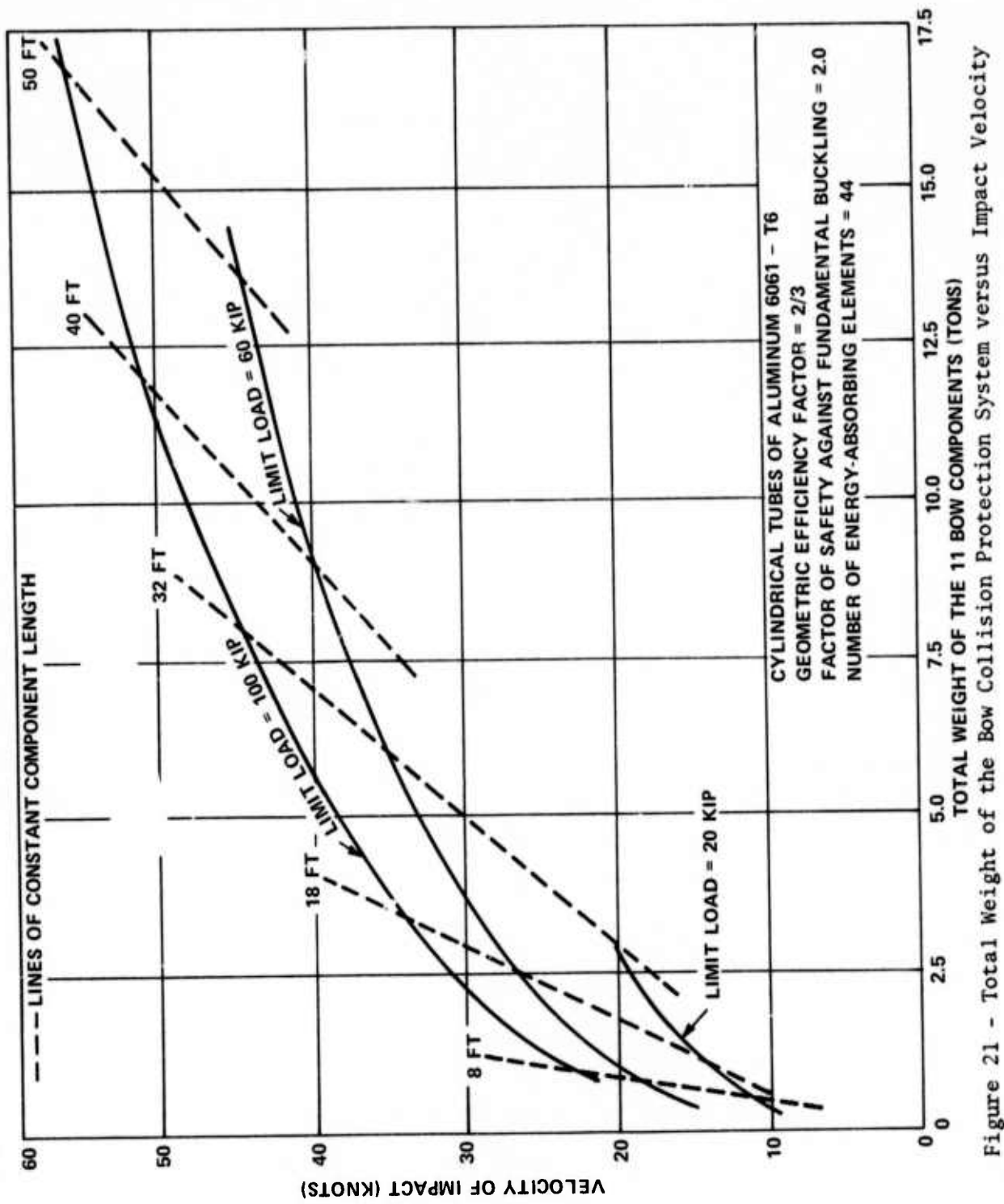


Figure 21 - Total Weight of the Bow Collision Protection System versus Impact Velocity

APPENDIX A
EXPERIMENTAL DATA

Data are presented for impact tests conducted on the ballistic pendulum facility and the drop tower facility at NSRDC. The data are acceleration time histories of the impacting masses. Since the mass is a constant, the records may be interpreted as force time histories as well when multiplied by the impacting weight. The weights of the ballistic pendulum mass and the drop tower vehicle mass are 837 and 729 lb, respectively. The records presented are only a sampling of the total data collected.

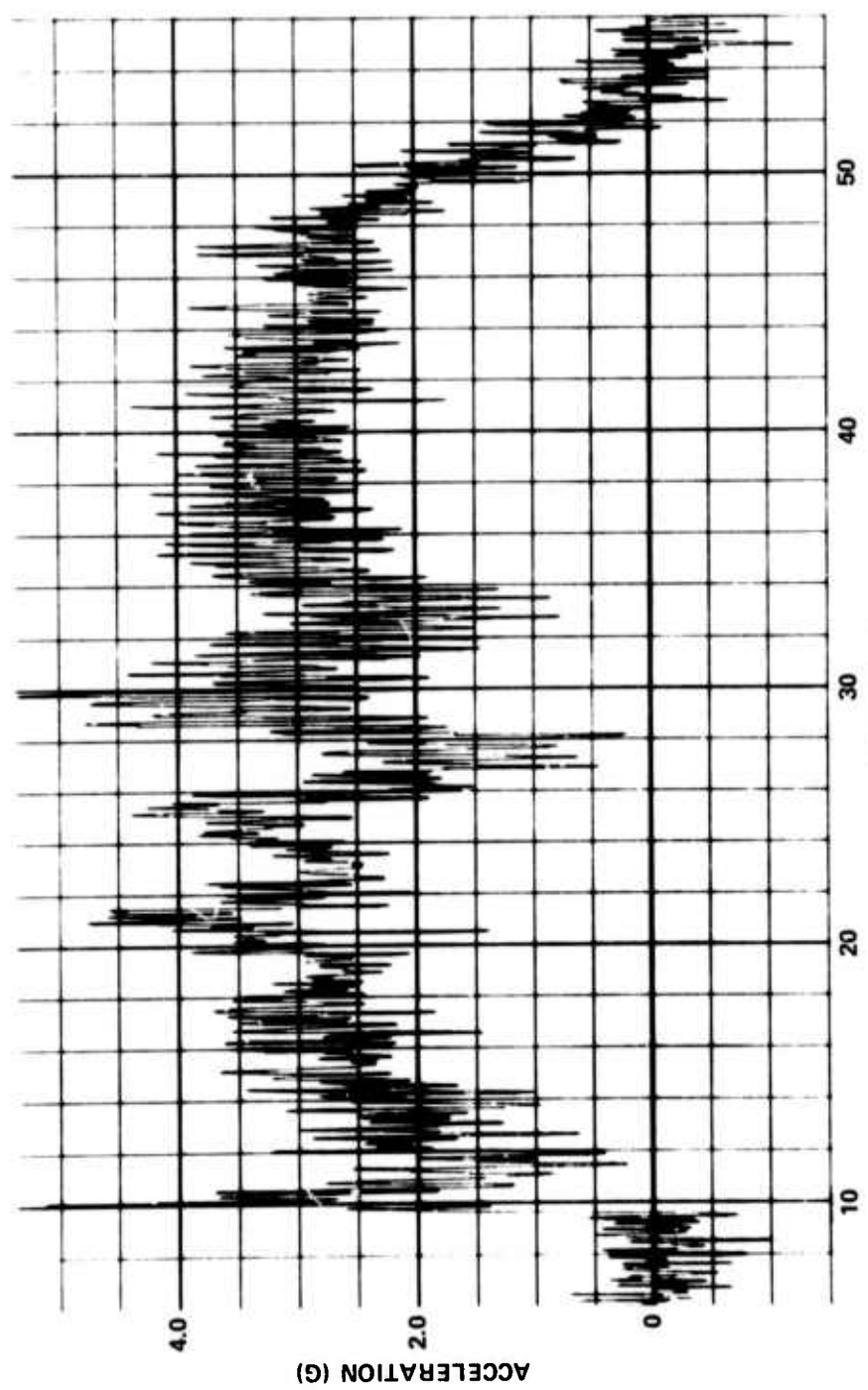


Figure A.1 - Ballistic Pendulum Test of Two-Element Configuration
(Cylindrical Tube with 1.0-in. OD and
0.035-in. wall, 31-in. drop height)

Figure A.2 - Drop Tower Tests of Two-Element Configurations

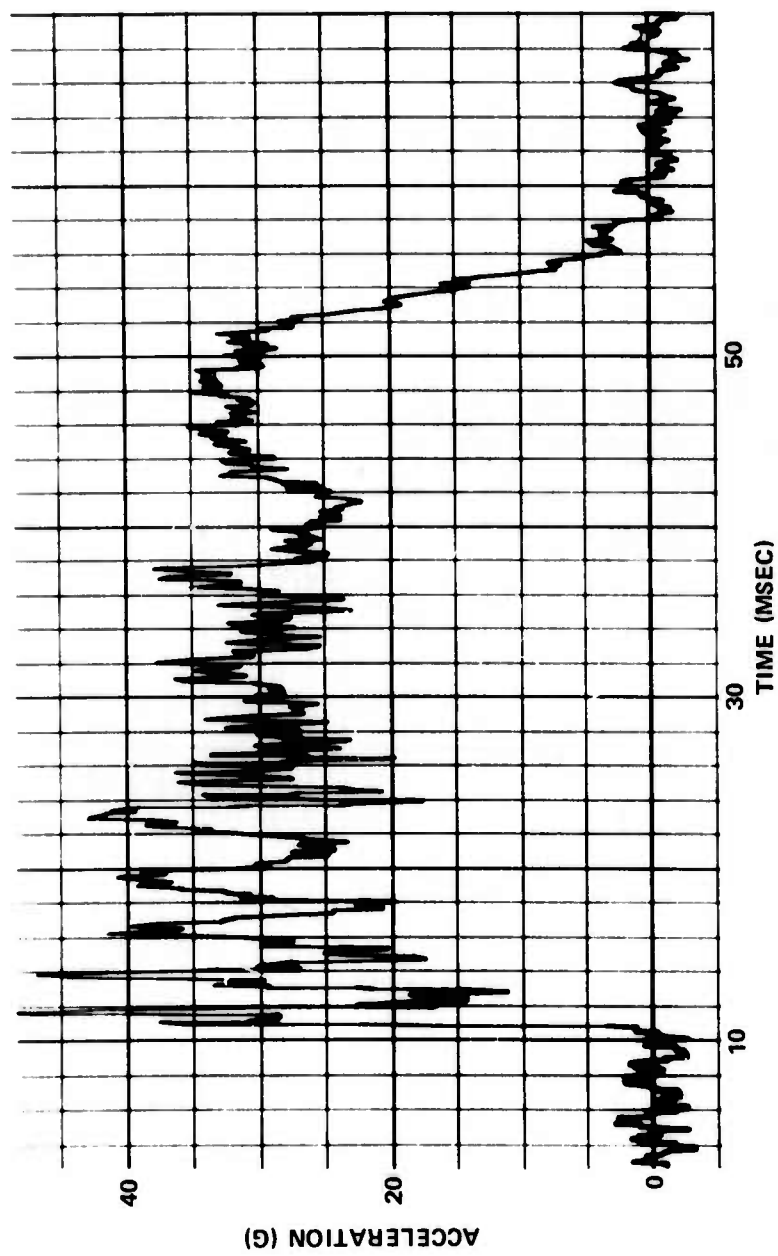


Figure A.2a - Cylindrical Tube with 2.0-Inch OD and 0.065-Inch Wall,
12-Foot Drop Height

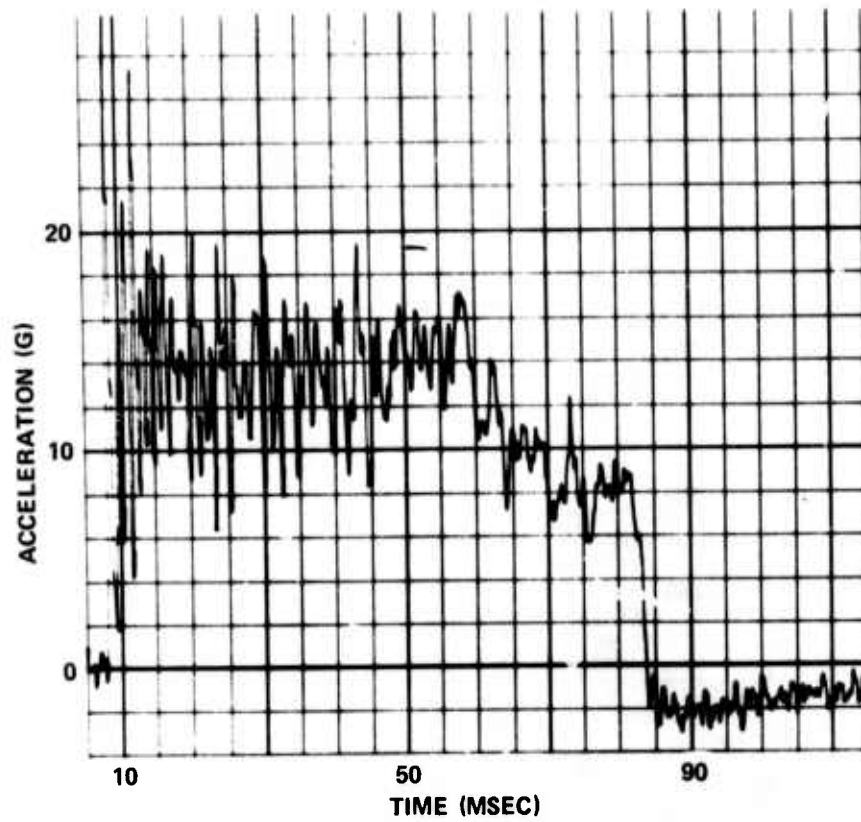


Figure A.2b - Cylindrical Tube with 2.0-Inch OD and 0.049-Inch Wall,
20-Foot Drop Height

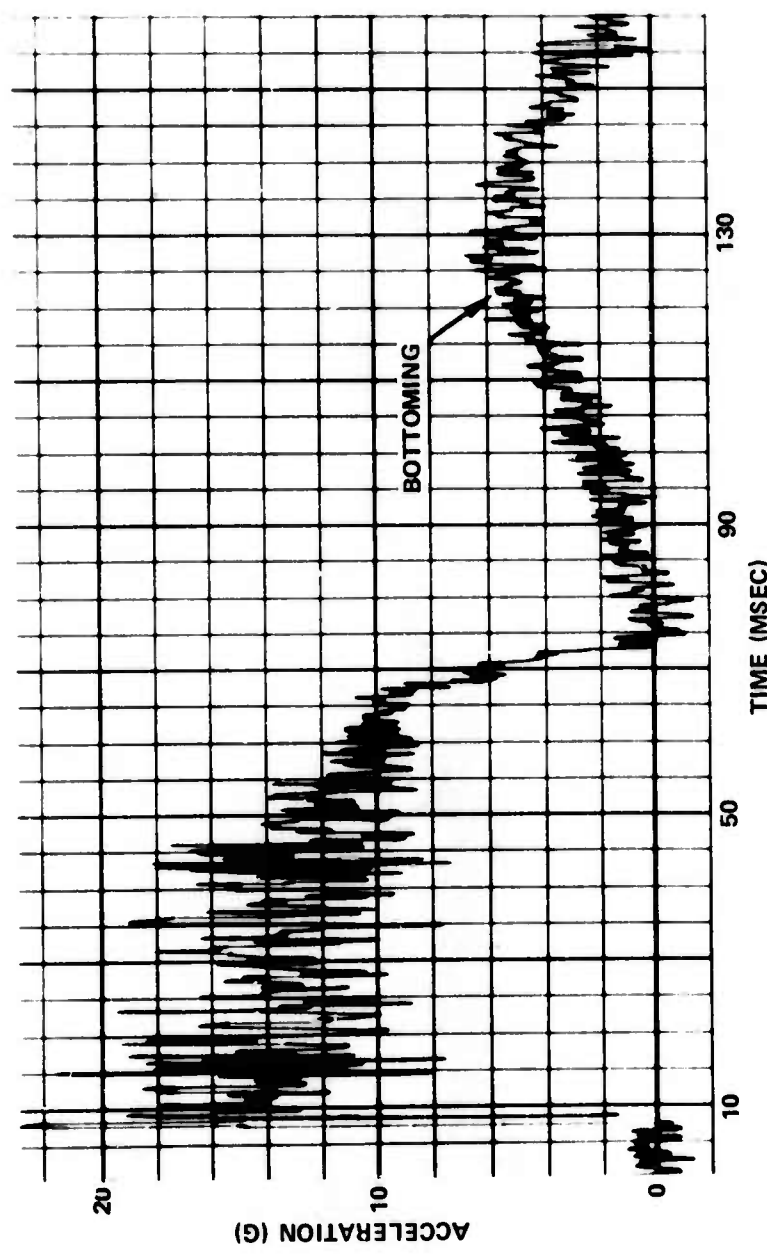


Figure A.2c - Cylindrical Tube with 3.0-Inch OD and 0.049-Inch Wall,
25-Foot Drop Height

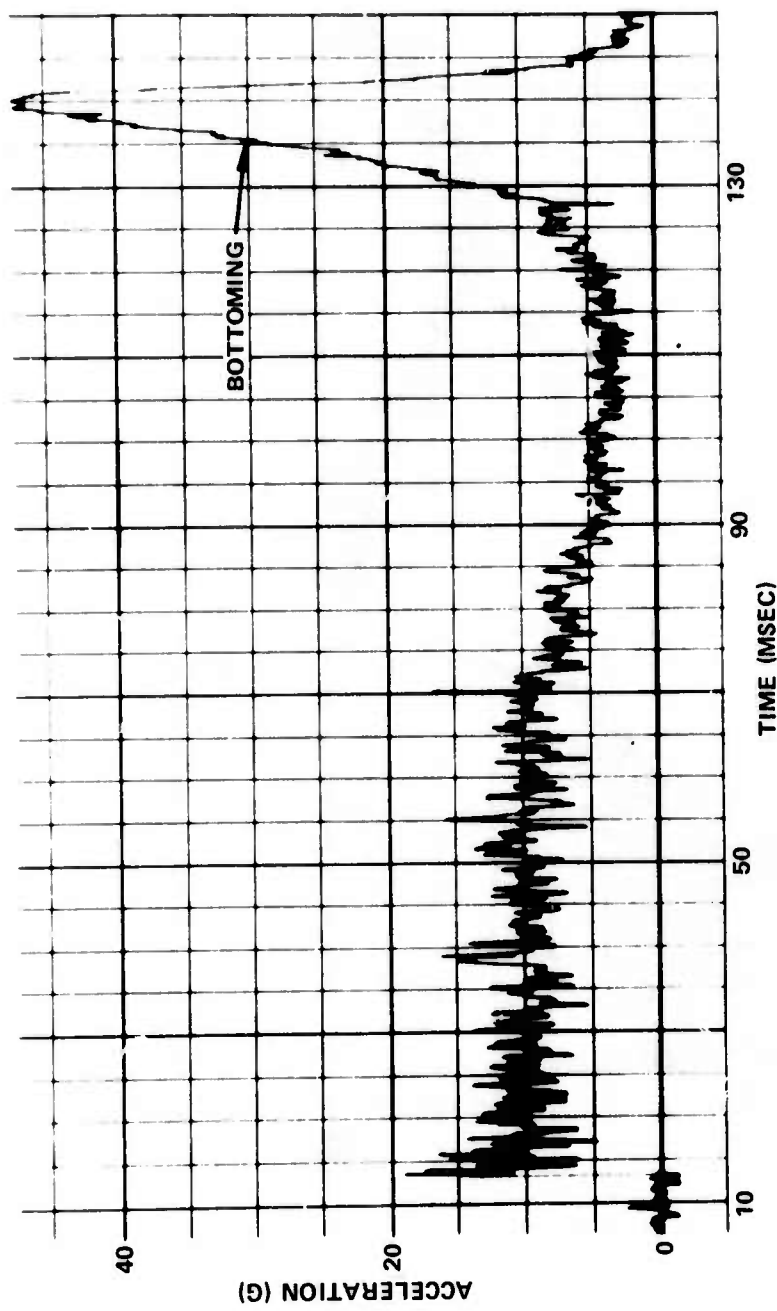


Figure A.2d - Cylindrical Tube with 5.5-Inch OD and 0.035-Inch Wall,
25-Foot Drop Height

Figure A.3 - Drop Tower Tests of Four-Element Configuration

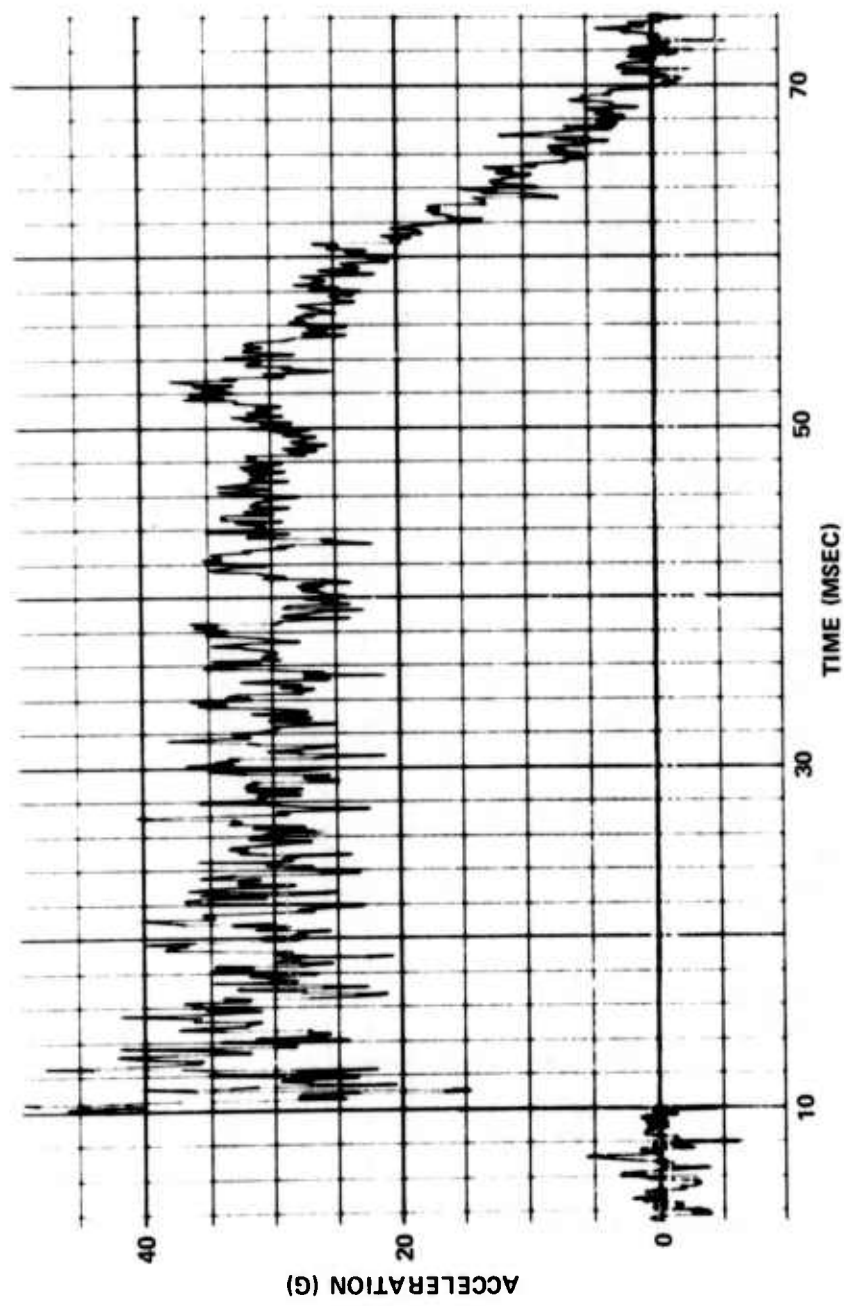


Figure A.3a - Cylindrical Tube with 3.5-Inch OD and 0.049-Inch Wall,
42.8-Foot Drop Height

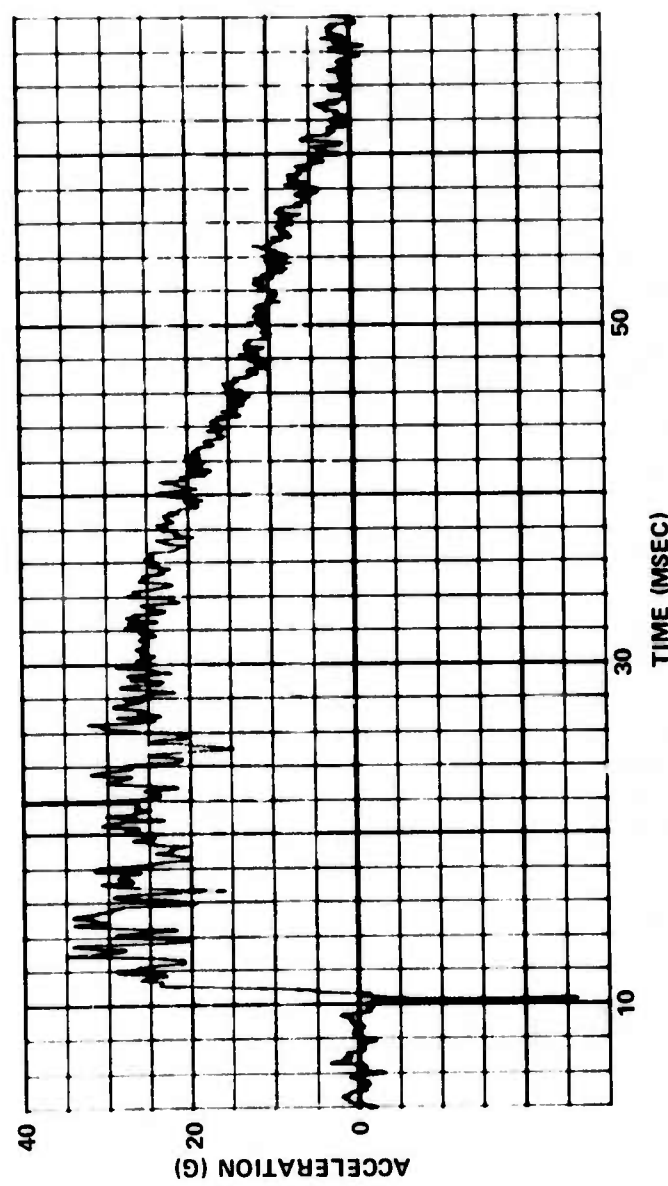


Figure A.3b - Cylindrical Tube with 3.5-Inch OD and 0.049-Inch Wall,
20-Foot Drop Height

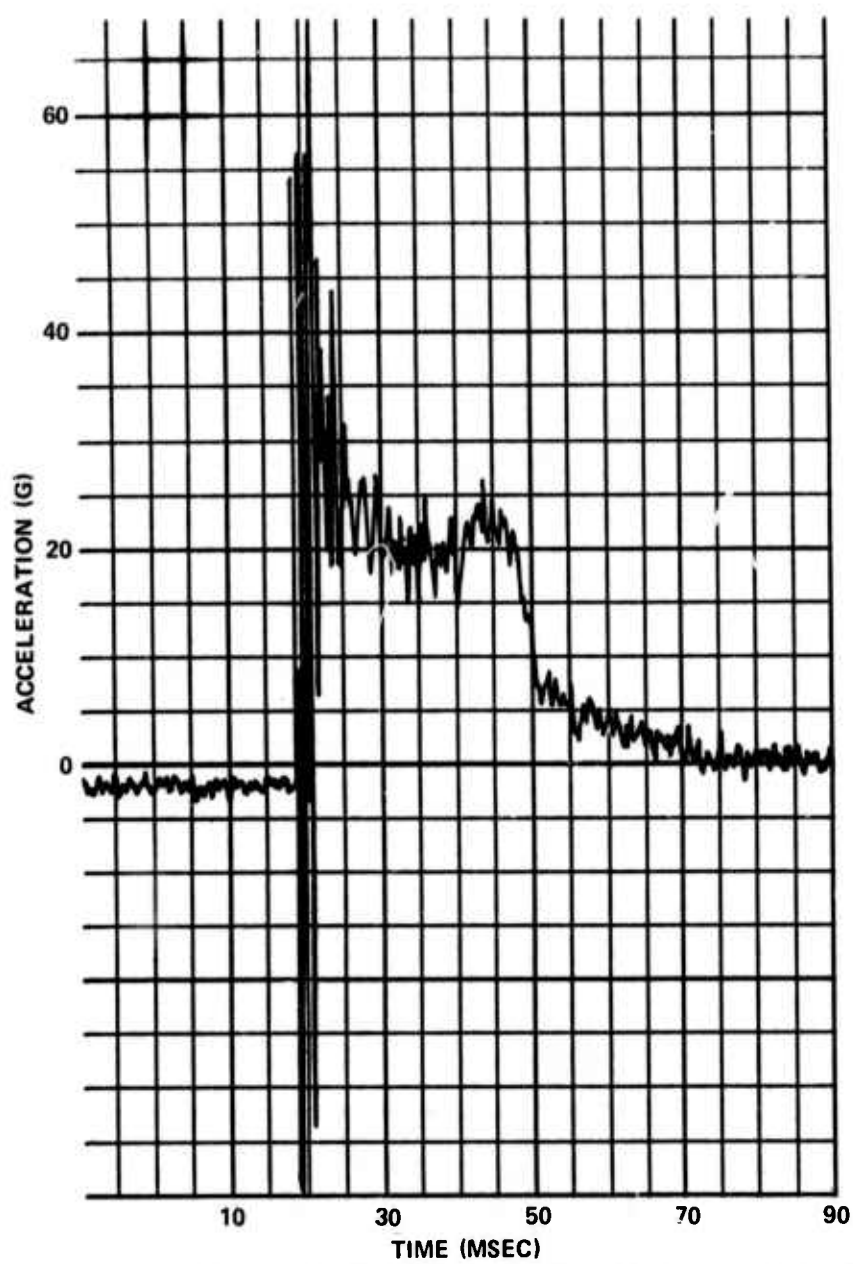


Figure A.4 - Drop Tower Test of Load Distribution System with Four-Element Configurations

(2.0-in. OD and 0.035-in. wall, 42-ft drop height)

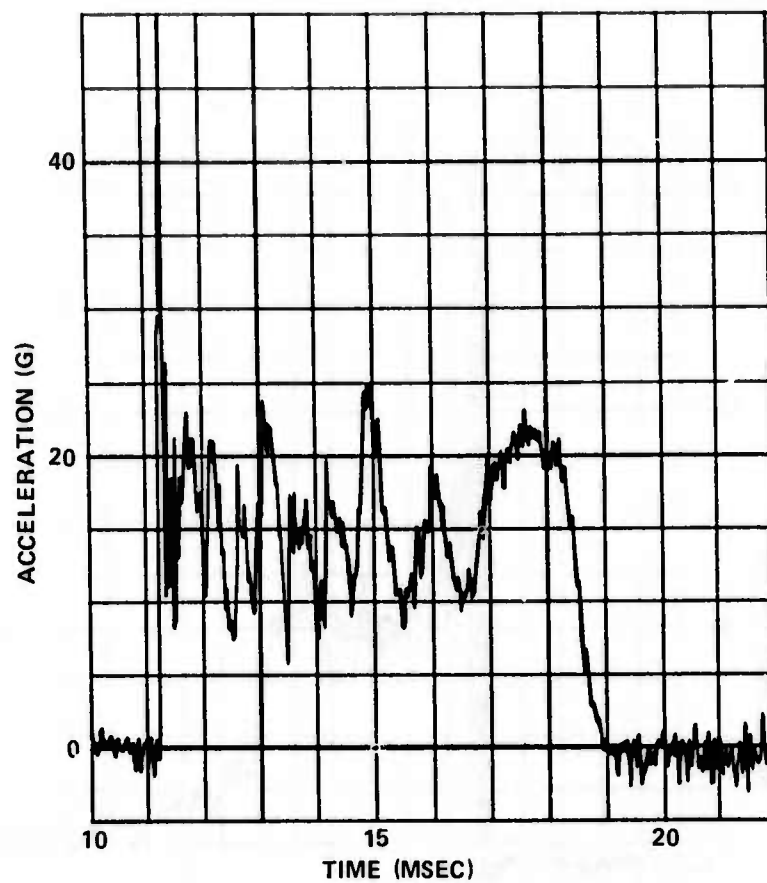


Figure A.5a - 4.0-Inch Square Tube with 0.125-Inch Wall, 25-Foot Drop Height

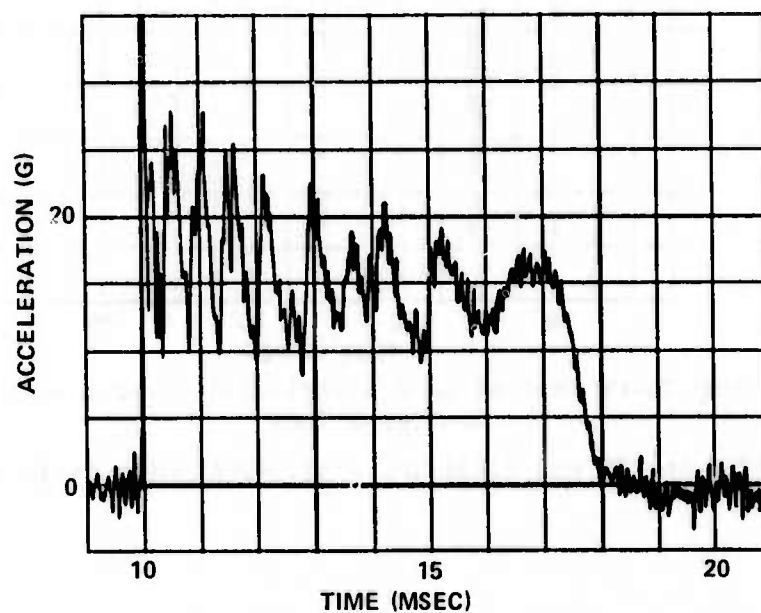


Figure A.5b - 3.0-Inch Square Tube with 0.125-Inch Wall, 27-Foot Drop Height

Figure A.5 - Drop Tower Tests of Single-Element Configuration

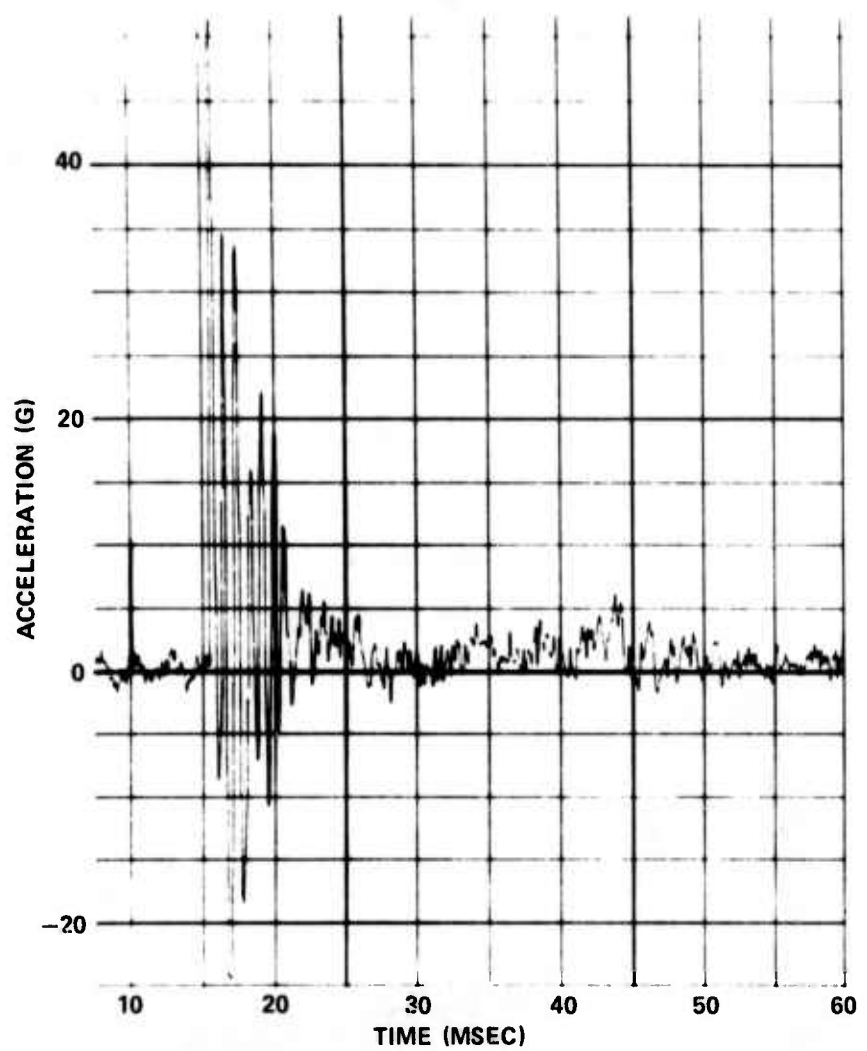


Figure A.6 - Drop Tower Test of Foam Core Sandwich Panel
(Drop Height of 12 ft)

Figure A.7 - Drop Tower Tests of Cylindrical Bumper Tubes

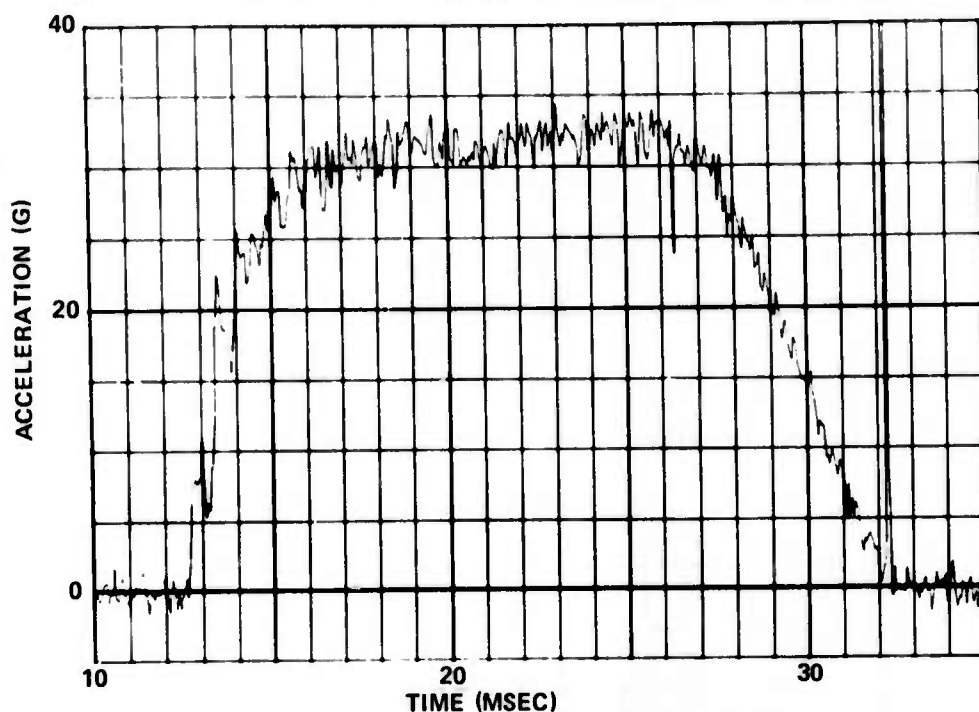


Figure A.7a - Tube with 3.0-Inch OD and 0.216-Inch Wall,
25-Foot Drop Height

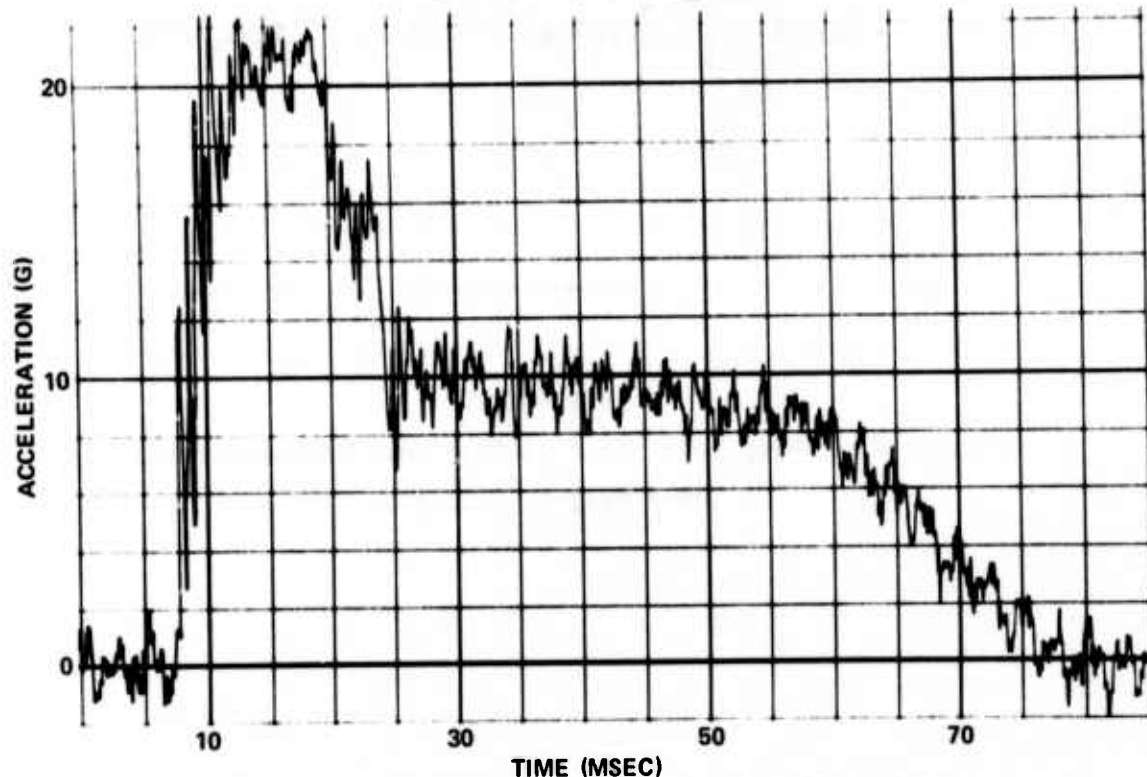


Figure A.7b - Tube with 6.0-Inch OD and 0.28-Inch Wall,
5.0-Foot Drop Height

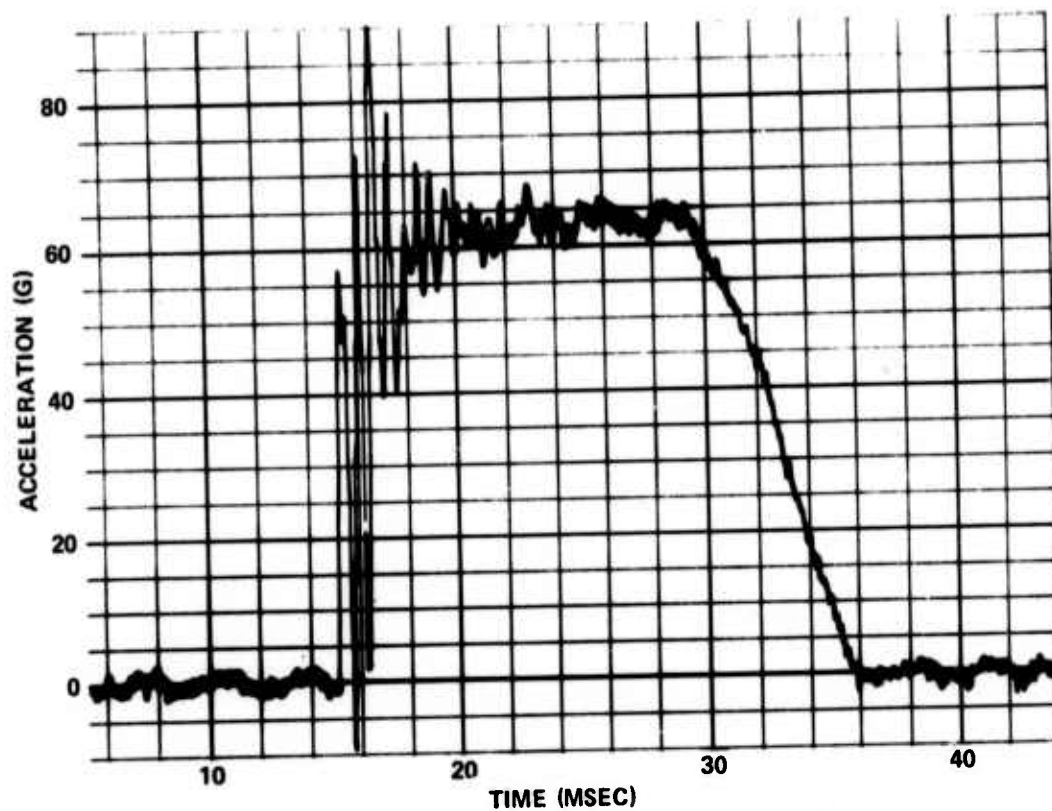


Figure A.7c - Tube with 8.0-Inch OD and 0.5-Inch Wall,
12-Foot Drop Height

APPENDIX B

SAMPLE TABLE OF PARAMETRIC DESIGN INFORMATION
(Allowable element crushing force = 20 kips)

PARAMETRIC OUTPUT ENERGY FACTOR	R/T	ELEMENT LIMIT LOAD (KIPS) IS		20.00	COMPONENT LIMIT LOAD (KIPS) IS		77.62	E/COMPONENT (IN-K/LB)
		THICKNESS (T)	LENGTH		ENERGY (IN-K)	WEIGHT		
.165	99.52	7.406	.0746	484.11	.61074E+04	167.66	36.4280	.24430E+05
.170	86.26	6.793	.0768	437.47	.55190E+04	147.05	37.5319	.22076E+05
.175	76.51	6.389	.0814	405.42	.51147E+04	132.38	38.6357	.20459E+05
.180	73.01	6.0374	.0832	360.10	.47953E+04	120.67	39.7396	.19101E+05
.185	68.74	5.613	.0846	358.86	.45273E+04	110.84	40.8435	.18109E+05
.190	65.26	5.589	.0856	340.44	.42949E+04	102.39	41.9474	.17100E+05
.195	62.31	5.391	.0865	324.13	.40892E+04	94.93	43.0512	.16357E+05
.200	59.76	5.213	.0872	309.49	.39044E+04	88.43	44.1551	.15618E+05
.205	57.51	5.051	.0878	296.20	.37367E+04	82.56	45.2590	.14947E+05
.210	55.49	4.902	.0883	284.03	.35833E+04	77.29	46.3629	.14333E+05
.215	53.67	4.765	.0888	272.83	.34420E+04	72.51	47.4668	.13768E+05
.220	52.01	4.637	.0892	262.47	.33312E+04	68.17	48.5706	.13245E+05
.225	50.47	4.517	.0895	252.83	.31697E+04	64.21	49.6745	.12759E+05
.230	49.06	4.404	.0898	243.84	.30762E+04	60.58	50.7784	.12355E+05
.235	47.74	4.298	.0900	235.42	.29700E+04	57.24	51.8623	.11860E+05
.240	46.50	4.198	.0903	227.52	.28703E+04	54.17	52.9662	.11461E+05
.245	45.35	4.133	.0905	220.08	.27765E+04	51.33	54.0900	.11105E+05
.250	44.25	4.012	.0907	213.16	.26679E+04	48.70	55.1939	.10752E+05
.255	43.22	3.926	.0908	206.43	.26643E+04	46.26	56.2976	.10417E+05
.260	42.24	3.844	.0910	200.15	.25550E+04	43.99	57.4017	.10100E+05
.265	41.31	3.765	.0912	194.19	.24499E+04	41.67	58.5055	.97995E+04
.270	40.42	3.690	.0913	188.53	.23705E+04	39.90	59.6094	.95139E+04
.275	39.57	3.617	.0914	183.15	.23106E+04	38.06	60.7133	.92422E+04
.280	38.75	3.549	.0916	178.02	.22458E+04	36.33	61.8172	.89333E+04
.285	37.97	3.481	.0917	173.12	.21841E+04	34.71	62.9211	.87364E+04
.290	37.22	3.417	.0918	168.45	.21251E+04	33.19	64.0249	.85006E+04
.295	36.50	3.354	.0919	163.98	.20686E+04	31.76	65.1286	.82751E+04
.300	35.80	3.295	.0920	159.71	.20140E+04	30.42	66.2327	.80593E+04

APPENDIX C
LISTING FOR COMPUTER PROGRAM COLIDE

```

PROGRAM COLIDE (INPUT,OUTPUT,TAPE5=INPUT,TAPE6=OUTPUT)
DIMENSION FP(30),XK(100),ROVT(100),T(30,100),R(30,100),XL(30,100),
1E(30,100),WGT(30,100),RATIO(30,100),BTITLE(6),EC(30,100),FC(30)
READ (5,6) (BTITLE(II),II=1,6)
6 FORMAT (6A10)
READ (5,7) FPLOW,FPHIGH,FPINC
FP(1)=FPLOW
NFP=30
NXK=100
DO 10 I=2,30
FPT=FP(I-1)+FPINC
IF (FPT-FPHIGH) 100,101,102
100 FP(I)=FPT
GO TO 10
101 FP(I)=FPT
NFP=I
GO TO 11
102 NFP=I-1
GO TO 11
10 CONTINUE
11 CONTINUE
READ (5,7) XKMIN,XKMAX,XKINC
XK(1)=XKMIN
DO 12 I=2,100
XKT=XK(I-1)+XKINC
IF (XKT-XKMAX) 103,104,105
103 XK(I)=XKT
GO TO 12
104 XK(I)=XKT
NXK=I
GO TO 13
105 NXK=I-1
GO TO 13
12 CONTINUE
13 CONTINUE
READ (5,7) SIGMA,ANGLE,FACSF,EFFGMY,EMOD,DENSE,NE
7 FORMAT (6F10.2,I10)
RANG=ANGLE*3.14159/180.
DO 30 J=1,NXK
XKT=XK(J)
TEMP=(XKT-0.16)/0.9107
30 ROVT(J)=- ALOG(TEMP)/0.0523
DO 9 IX=1,NFP
9 FC(IX)=FP(IX)*NE*COS(RANG)
DO 20 I=1,NFP
FPT=FP(I)
DO 40 J=1,NXK
XKT=XK(J)
ROT=ROVT(J)
T(I,J)=SQRT(FPT/(XKT*SIGMA*6.28318*ROT))
R(I,J)=T(I,J)*ROT
XL(I,J)=3.14159*SQRT(EMOD*3.14159*R(I,J)**3.*T(I,J)/(FPT*FACSF))
E(I,J)=EFFGMY*FPT*COS(RANG)*XL(I,J)*COS(RANG)
EC(I,J)=E(I,J)*NE
WGT(I,J)=3.14159*2.0*R(I,J)*T(I,J)*DENSE*XL(I,J)

```

```

RATIO(I,J)=E(I,J)/HGT(I,J)
40 CONTINUE
20 CONTINUE
  WRITE (6,200) (BTITLE(K),K=1,6),SIGMA,ANGLE,NE,FACSF,EFFGMY,
  1EMOD,DENSE
200 FORMAT (1H1,10X,18H INPUT PARAMETERS //2X,6A10//22H YIELD STRESS (
  1KSI) = ,F12.2
  1/52H ANGLE OF EACH ELEMENT TO THE LOAD LINE (DEGREES) = ,F12.2/
  636H NUMBER OF ELEMENTS PER COMPONENT = ,I2/
  241H FACTOR OF SAFETY ON THE BUCKLING LOAD = ,F5.2/
  352H EFFICIENCY FACTOR FOR THE CONFIGURATION GEOMETRY = ,F5.2/
  431H MODULUS OF ELASTICITY (KSI) = ,F12.2/31H MATERIAL DENSITY (LB/
  5CU-IN) = ,F12.2//)
  WRITE (6,201) FPLOW,FPHIGH,FPINC,XKMIN,XKMAX,XKINC
201 FORMAT (29H MINIMUM LIMIT LOAD (KIPS) = ,F12.2/29H MAXIMUM LIMIT L
  LOAD (KIPS) = ,F12.2/31H LIMIT LOAD INCREMENT (KIPS) = ,F12.2//)
  225H MINIMUM ENERGY FACTOR = ,F6.3/25H MAXIMUM ENERGY FACTOR = ,F6.
  33/27H ENERGY FACTOR INCREMENT = ,F6.3///)
  DO 50 I=1,NFP
  WRITE (6,202) FP(I),FC(I)
202 FORMAT (1H1,3X,50H PARAMETRIC OUTPUT ELEMENT LIMIT LOAD (KIPS) I
  1S ,F12.2,34H COMPONENT LIMIT LOAD (KIPS) IS ,F12.2
  1//113H ENERGY FACTOR R/T RADIUS (R) THICKNESS (T)
  2 LENGTH ENERGY (IN-K) WEIGHT E/W (IN-K/LB),2X,19H E/COM
  1PONENT (IN-K)//)
  WRITE (6,203) (XK(J),ROVT(J),R(I,J),T(I,J),XL(I,J),E(I,J),HGT(I,J)
  1,RATIO(I,J),EC(I,J),J=1,NXK)
203 FORMAT (3X,F6.3,6X,F10.2,5X,F10.3,4X,F10.4,4X,F10.2,3X,E11.5,4X,
  1F10.2,4X,F10.4,7X,E11.5//)
50 CONTINUE
  WRITE (6,205)
205 FORMAT (1H1//16H END OF PROBLEMS)
STOP
END

```

REFERENCES

1. Pounder, E. R., "Physics of Ice," Pergamon Press, New York (1965).
2. Weeks, W. and A. Assur, "Mechanical Properties of Sea Ice," Cold Regions Research and Engineering Laboratory, Hanover, New Hampshire, Monograph II-C3 (Sep 1967).
3. Hirsch, A. E., "Man's Response to Shock Motions," David Taylor Model Basin Report 1797 (Jan 1964).
4. Mahone, R. M., "Man's Response to Ship Shock Motions," David Taylor Model Basin Report 2135 (Jan 1966).
5. Gilbert, W. E., "Collision Protection for the Arctic Surface Effect Vehicle (ASEV)," NSRDC Report 3885 (Feb 1973).
6. Goppa, A., "On the Mechanism of Buckling of a Circular Cylindrical Shell Under Longitudinal Impact," General Electric Company, Missile and Space Vehicle Department, Technical Information Series R60SD494 of the Space Sciences Laboratory (1960).
7. Howe, J. T., "Theory of High-Speed-Impact Attenuation by Gas Bags," NASA, Ames Research Center, NASA-TN-D-1298 (Apr 1962).
8. Timoshenko, S. P. and J. M. Gore, "Theory of Elastic Stability," Second Edition, McGraw-Hill Book Company, New York (1961), pp. 1-8.
9. Perrone, N., "Impulsively Loaded Strain-Hardened Rate-Sensitive Rings and Tubes," Report 10 under National Science Foundation Grant GK782, Catholic University of America (Apr 1969).
10. Morton, A. G. S. and M. Silvergleit, "Review of Candidate Structural Materials for an Arctic Surface Effect Vehicle," NSRDC Report 3573 (May 1972).
11. Borg, S. F. and J. J. Gennaro, "Advanced Structural Analysis," D. Van Nostrand Company, Inc., New York, New York (1959), pp. 80-83.

INITIAL DISTRIBUTION

Copies	Copies
1 ARPA, CDR B. K. Hannula	1 Dr. M. G. Bekker
1 Army Res Office Dr. V. Zadnik	1 Bell Aerospace, H. K. Hite
1 AMERDC, J. Sargent	1 Boeing Aerospace, R. Miller
1 ACRRDL, Dr. K. F. Sterrett	1 Booz-Allen, C. F. Willard
1 ASTSECNAV (R&D) CDR A. Smith	1 Daedalean Assoc, A. Thiruvengadam
1 HQS MARCORPS DCS (RD&S)	1 Goodyear Aerospace, W. B. Cross
1 CHONR (Code 415)	1 Grumman, R. Munz
1 USNA Mech Engr Dept J. F. Sladky	1 Oceanics, P. Kaplan
1 MCDEC Devel Cen	1 Robert S. Ross
2 NAVSHIPS 1 SHIPS 031 1 SHIPS 03Z2 J. L. Schuler	1 SCI APPLI, Dr. C. Whittenberry
1 AIR (Code 03)	1 UA Hamilton Stan, H. E. Deabler

CENTER DISTRIBUTION

Copies	Code
1 NAVSEC (Code 6110.01)	1 1100
1 USAFA, R. W. Gallington	15 1130 J. U. Kordenbrock
1 AFFDL/FEM, Dr. K. H. Digges	1 1150
1 SAMSO XRTB LCOL N. F. Finnegan	1 1180
1 HQS COGARD Off Res & Dev	1 1572
1 HQS NASA	1 1610
2 DOT 1 Res & Technol 1 High Speed Ground Trans	1 1700
1 Cornell, S. F. Shen	1 1730
1 JHU APL, F. C. Paddison	1 1731
1 U Washington, G. Gray	2 1735 1 R. G. Allen 1 A. J. Furio, Jr.
1 Aero-Jet Gen, Dr. L. Shenfil	1 1740
1 Arctic Inst North Amer, R. Faylor	23 1745 1 W. R. Conley 20 W. E. Gilbert 1 H. P. Gray 1 E. T. Habib
2 Aerospace Sev 1 K. T. Scott 1 C. L. Crews	

Copies Code

2	1747
	1 A. P. Misovec
	1 A. R. Willner
1	1770
1	2721
1	2803
1	9400

UNCLASSIFIED

Security Classification

DOCUMENT CONTROL DATA - R & D

(Security classification of title, body of abstract and indexing annotation must be entered when the overall report is cleared filed)

1. ORIGINATING ACTIVITY (Corporate author)		2a. REPORT SECURITY CLASSIFICATION	
Naval Ship Research and Development Center Bethesda, Md. 20034		2b. GROUP	
3. REPORT TITLE EMPIRICAL DESIGN OF PERIPHERAL COLLISION PROTECTION STRUCTURE FOR THE ARCTIC SURFACE EFFECT VEHICLE			
4. DESCRIPTIVE NOTES (Type of report and inclusive dates)			
5. AUTHOR(S) (First name, middle initial, last name) William E. Gilbert			
6. REPORT DATE December 1973	7a. TOTAL NO. OF PAGES 85	7b. NO. OF REFS 11	9a. ORIGINATOR'S REPORT NUMBER(S) 4232
8a. CONTRACT OR GRANT NO.	9b. OTHER REPORT NO(S) (Any other numbers that may be assigned this report)		
b. PROJECT NO. c. ARPA Order 1676, Program Code ON10	d. Work Unit 1130-600		
10. DISTRIBUTION STATEMENT Distribution limited to U.S. Government agencies only; Test and Evaluation Info., Dec 1973. Other requests for this document must be referred to NAVSHIPRANDCEN, Code 1700.			
11. SUPPLEMENTARY NOTES	12. SPONSORING MILITARY ACTIVITY Advanced Research Projects Agency (ARPA)		
13. ABSTRACT Collision protection for the Arctic surface effect vehicle (ASEV) was investigated and a collision protection philosophy developed for peripheral protection. Several peripheral protection schemes were evaluated and the most promising further developed and evaluated in a collision test program. A procedure is proposed for the design of discrete collision protection elements, and a computer program is documented which is a useful design tool when thin-wall tubes serve as the energy-absorbing elements.			

DD FORM 1473 (PAGE 1)
1 NOV 65

S/N 0101-807-6801

UNCLASSIFIED

Security Classification

UNCLASSIFIED
Security Classification

14 KEY WORDS	LINK A		LINK B		LINK C	
	ROLE	WT	ROLE	WT	ROLE	WT
Arctic Surface Effect Vehicle Collision with Ice Obstacles Impact Design Energy Absorption Candidate Energy-Absorbing Elements Inextensional Buckling Gross Buckling (Euler Mode) Load Distribution System Computer Program COLIDE						